

Dear Dr. Ervens,

Thank you very much for your patience and help! Thank you for permission for an extension of the resubmission of the revised manuscript (Ms. Ref. No.:acp-2016-1183). Based on the critical comments of the two reviewers, we have made a substantial revision to our manuscript, including reanalyzing the data, supplementing the model results, enhancing our discussion and changing the references. Most figures and tables have been revised. Additionally, we added 8 supporting files. Due to the substantial changes, the contributions of the authors of this manuscript have changed; hence, we have added two authors and revised the title of the revised manuscript. Detailed item-by-item responses to the comments of Referee #2 are listed below.

Best regards,

Yours sincerely,

Jianhua Qi

Reply to Interactive comment on "The concentration, source apportionment and deposition flux of atmospheric particulate inorganic nitrogen during dust events" by Jianhua Qi et al. Anonymous

Referee #2 Received and published: 27 March 2017

General comments: This paper attempts to study the impact of spring time dust storms in the Chinese deserts on the atmospheric concentration and deposition of inorganic nitrogen (IN) in the coastal Yellow Sea location. The study uses 4 years of particulate matter measurements and their chemical composition to understand how different types of dust storms can affect the abundance of inorganic nitrogen and calculate dry deposition of IN to the coastal Yellow Sea. This type of work is relevant since atmospheric deposition of nutrients and its implications is not a well understood topic and can be important for the regions that receive high atmospheric input like the Yellow Sea. However, the authors have not made best use of the data. There needs to be significant improvement in data interpretation and much more analysis needs to be done to support the main results. I would thus recommend a resubmission and see if there is any substantial improvement in the manuscript. My main comments are given below.

Reply: Thank you for the suggestion. We have reanalyzed the data and supplemented the modeling results using a 3-D air quality model to support the main results in the revised version. We have added "Theoretical analysis of three categories" and "The impact of dust on nitrogen dry deposition flux under anthropogenic activity" to the discussion section. Some figures have been redrawn, and some references have been updated. The data interpretation and the writing have also been improved. In brief, we have made substantial improvements to our manuscript.

Q1.First of all, the manuscript needs an overall improvement in writing. Not sufficient care has been given to the details and there are parts which are difficult to follow. I will provide some examples later, but there are many such cases of improper and awkward sentence constructions. Second, on what basis are these dusty and non-dusty days decided? More information are needed to show whether the dust storms originating from the deserts are actually passing over the measurement site and it is not the locally produced soil dust in cases of the days with low TSP values. Satellite aerosol products and meteorological data can be used to support this. Again later AI concentration is used to identify dust weather (lines 171-172). Please provide a clear definition of dust days and maintain that throughout the manuscript.

Reply: We have revised all sections of this manuscript, especially the sections "Experimental Method" and "Results and Discussion", to provide detailed methods and a logical analysis of the data. The discussion was revised substantially. Additionally, the writing has also been improved by a native English speaker.

In this study, a dust event was defined according the definition adopted in regulations of surface meteorological observation in China (CMA, 2004; Wang et al., 2008) and was identified based on the meteorological record information from Meteorological Information Comprehensive Analysis and Process System (MICAPS) of China Meteorological Administration. The sampling information is listed in the Table 1. Based on the forecast, we also collected aerosol particle samples immediately before or after the dust event for comparison. The post-dust event samples were collected under clear and sunny weather conditions and at low mass concentrations of PM₁₀.

All air mass trajectories showed that dust storms originated from deserts or Gobi and passed over the measurement site. More information on the dust events has been added to Tables 1 and 4. According to the suggestion, we tried to obtain aerosol particle concentrations using satellite aerosol products; however, the daily satellite data were incomplete. Therefore, we have included modeled dust concentrations over East Asia based on the CFORS model by Uno et al. (2003) (<http://www-cfors.nies.go.jp/>) and the PM10 modeling results for each dust event using a 3-D air quality model to support our analysis in the revision. The model results for each event are shown in Fig. 2 and Fig.S3. Based on Fig. 2, we found that the Sample 20110418 was mainly affected by local blowing dust. To focus on the impact of long-range transported dust on aerosol samples in downwind areas, this sample 20110415 was not included in the analysis and discussion in later sections.

As the reviewer suggested, the samples can be affected by local soil dust. Therefore, we used the criterion method of total Al concentration in TSP samples proposed by Hsu et al. (2008) to confirm that our samples originated from the sandy sources, as proposed in the previous version of this manuscript. We have added the distribution of hourly dust concentrations modeled over East Asia by the CFORS model for dust events in the revised version. The model results show the dust occurrence and transport patterns, thereby providing much more information than the Al criteria method. Therefore, we revised this section and replaced the Al criteria method with the model results in the revised manuscript.

Table 1. Sampling information for the aerosols samples collected at the Baguanshan site in the coastal region of the Yellow Sea.

Sampling Year	Sample category	Sampling number	Sampling time	Weather characteristics	
2008	Samples on dust days	20080301	From 13:22 a.m. to 17:22 p.m. on Mar. 1st	Floating dust ^a	
		20080315	From 13:21 a.m. to 17:21 p.m. on Mar. 15 th	Floating dust	
		20080425	From 13:14 a.m. to 17:14 p.m. on Apr. 25th	Floating dust	
		20080528	From 11:38 a.m. to 15:38 p.m. on May 28th	Floating dust	
		20080529	From 10:15 a.m. to 12:15 p. m. on May 29th ^b	Floating dust	
	Samples on non-dust days	20080316	From 13:00 a.m. to 17:00 p.m. on Mar. 16th	Sunny day	
		20080424	From 13:00 a.m. to 17:00 p.m. on Apr. 24th	Sunny day	
		20080522	From 13:00 a.m. to 17:00 p.m. on May 22nd	Cloudy day with mist	
	2009	Samples on dust days	20090316	From 8:25 a.m. to 12:25 p.m. on Mar. 16th	Floating dust
		Samples on non-dust days	20090306	From 13:00 a.m. to 17:00 p.m. on Mar. 6th	Sunny day

2010	Samples on dust days	20100315	From 11:30 a.m. to 15:30 p.m. on Mar. 16th	Mist after dust	Floating dust
		20100320	From 10:30 a.m. to 14:30 p.m. on Mar. 20th		Floating dust
		20100321	From 10:30 a.m. to 14:30 p.m. on Mar. 21st		Floating dust
	Samples on non-dust days	20100324	From 11:30 a.m. to 15:30 p.m. on Mar. 24th		Sunny day
2011	Samples on dust days	20110319	From 12:00 a.m. to 16:00 p.m. on Mar. 19th		Floating dust
		20110415	From 12:00 a.m. to 16:00 p.m. on Apr. 15th		Floating dust
		20110418	From 12:25 a.m. to 16:25 p.m. on Apr. 18th		Floating dust ^c
		20110501	From 12:10 a.m. to 16:10 p.m. on May 1st		Floating dust
	20110502	From 16:00 a.m. to 20:00 p.m. on May 2nd		Floating dust	
	Samples on non-dust days	20110308	From 12:00 a.m. to 16:00 p.m. on Mar. 8th		Sunny day
		20110416	From 12:00 a.m. to 16:00 p.m. on Apr. 16th		Sunny day
20110523		From 12:00 a.m. to 16:00 p.m. on May 23rd		Sunny day	

^aNote that one exterior dust sample was collected on March 1 when no dust was recorded by the MICAPS. However, the MICAPS information indeed showed dust events in China on March 1. The modeled spatial distribution of the PM₁₀ mass concentration for this dust event on March 1 implies that the sample should be classified as a dust sample. The supporting figure is Fig. S1.

^b The sampling duration was reduced to only 2 hrs because of extremely high particle loads.

^cNote that one exterior dust sample was collected on April 18 when no dust was recorded by the MICAPS. However, blowing dust occurred and was recorded on April 17 by the Sand-dust weather almanac 2011 (CMA, 2011). The modeled spatial distribution of the PM₁₀ mass concentration for this dust event on April 18 implies that the sample should be classified as a dust sample. The supporting figure is Fig. S2

Table 4. Average concentrations of inorganic nitrogen, TSP, NO_x, Relative Humidity (RH) and air temperature for each Category in aerosol samples in Qingdao

	Sample number	TSP μg·m ⁻³	NO ₃ ⁻ μg·m ⁻³	NH ₄ ⁺ μg·m ⁻³	RH %	T °C	NO _x μg·m ⁻³	Summary
Category 1	20080301	527	20.5	12.7	57	7.0	36	IN concentration on dust days higher than that on ND days
	20080315	410	19.5	29.9	62	11.0	59	
	20090316	688	15.9	17.2	27	16.0	75	

	20100321	519	16.5	9.4	51	8.8	76	
	20110502	810	21.0	11.0	49	17.7	62	
Category 2	20080425	622	6.8	2.0	30	18.0	40	IN concentration on dust days lower than that on ND days
	20080528	2579	9.2	2.7	17	27.0	34	
	20080529	2314	17.5	4.8	60	20.0	29	
	20110319	939	12.3	9.4	16	12.6	93	
	20110501	502	4.5	5.3	23	21.6	66	
Category 3	20100315	501	5.4	4.3	30	7.2	73	NO ₃ ⁻ concentration on dust days lower than that on ND days; NH ₄ ⁺ close to that on ND days
	20100320	3857	5.5	3.4	35	10.6	92	
	20110418	558	3.8	6.6	33	12.6	47	
Non-dust ^a	20080316	225	12.6	8.4	28	11.0	60	
	20080424	137	21.7	7.2	49	18.0	53	
	20080522	206	27.4	16.6	78	20.0	60	
	20090306	94	2.9	3.0	29	7.00	51	
	20100324	275	7.2	2.4	23	9.0	82	
	20110308	194	13.0	13.1	20	11.5	111	
	20110416	252	5.6	5.4	26	14.1	55	
	20110523	224	15.2	10.2	42	20.6	49	

^a The corresponding ND day for each dust event see Table 1.

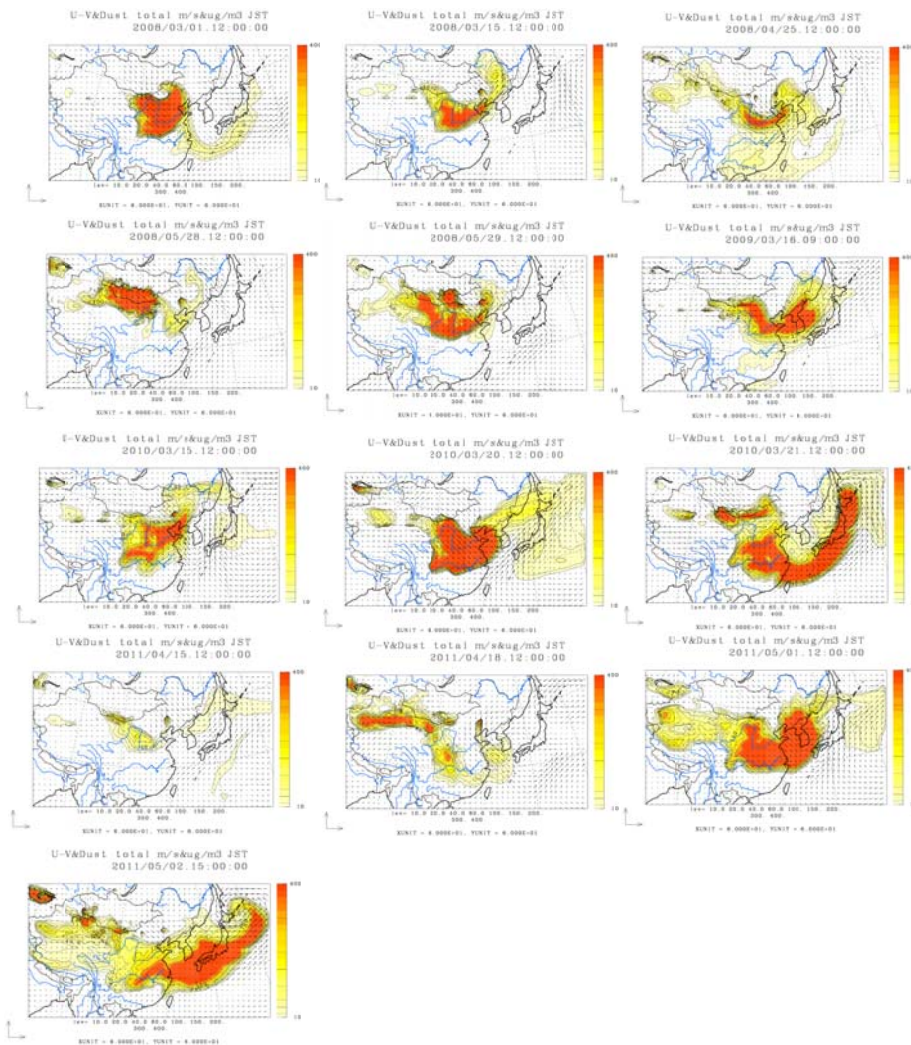


Figure 2. Modeled dust concentrations over East Asia by CFORS model during each dust sampling day from 2008 to 2011 (<http://www-cfors.nies.go.jp/>). (The figures show the modeled dust concentration in the middle of each sampling duration). No data are available for Mar. 19, 2011, because of the earthquake in Japan. Hourly PM10 concentrations were modeled by the WRF-CMAQ model for each sampling day, and the results are shown in Fig. S3.

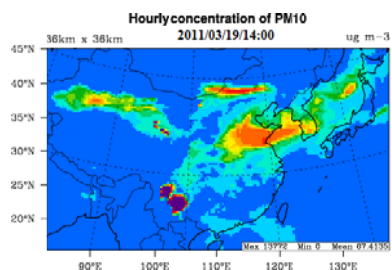


Figure S3. Hourly PM10 concentration in China modeled by the WRF-CMAQ model for Sample 20110418 (The figure shows the modeled PM10 concentration at the middle of the sampling

period).

CMA: Regulations of Surface Meteorological Observation, China Meteorological Press, Beijing, 154–156, 2004.

CMA: Sand-dust weather almanac 2011, China Meteorological Press, Beijing, 36-53, 2013.

Hsu, S. C., Liu, S. C., Huang, Y. T., Lung, S. C. C., Tsai, F., Tu, J. Y., and Kao, S. J.: A criterion for identifying Asian dust events based on Al concentration data collected from northern Taiwan between 2002 and early 2007, *J. Geophys. Res-Atmos.*, 113, 1044-1044, 2008.

Uno, I., Carmichael, G. R., Streets, D. G., Tang, Y., Yienger, J. J., Satake, S., Wang, Z., Woo, J. H., Guttikunda, S., Uematsu, M., Matsumoto, K., Tanimoto, H., Yoshioka, K., and Iida, T.: Regional chemical weather forecasting system CFORS: Model descriptions and analysis of surface observations at Japanese island stations during the ACE-Asia experiment, *J. Geophys. Res-Atmos.*, 108, 1147-1164, 2003.

Wang, Y. Q., Zhang, X. Y., Gong, S. L., Zhou, C. H., Hu, X. Q., Liu, H. L., Niu, T., and Yang, Y. Q.: Surface observation of sand and dust storm in East Asia and its application in CUACE/Dust, *Atmos. Chem. Phys.*, 8, 545-553, 2008.

Q2. The authors have divided dusty days into 3 categories based on inorganic nitrogen (IN) concentrations relative to the non dust (ND) days. They are reporting that in some cases IN concentrations are more than the ND days, in some cases IN concentration are less than the ND days and in some cases nitrate concentration on dust days are less than ND days while ammonium concentrations on dust days are more compared to ND days. Next, the authors are reporting that sand from Duolun (which is a source for dust storms affecting the Yellow Sea region) is poor in nitrate and ammonium content. First of all, trajectory analysis does not seem to point that coastal Yellow Sea region is only affected by dust originating from Duolun region. There are many other dust sources over which the trajectories are passing. And if Duolun is deficient in IN you need to provide a detailed discussion on the possible sources of IN in dust sampled from the coastal region of the Yellow Sea and about the mixing of anthropogenic aerosols with the dusty air mass. The authors have related the 3 cases of IN in dust samples to the wind speed concluding that when wind speed is less IN concentration increased and vice versa . I am not clear how this conclusion is arrived at, especially, with only 5 cases for $IN < ND$. Foreexample, in Table 5 sample number 110501 NO_3^- and NH_4^+ concentrations are low and the wind speed is also low. Again, sample 080315 has higher NO_3^- and NH_4^+ concentrations at higher wind speed. What is the rationale of using wind speed of 40.5km/h in this study and how is this threshold derived? I would suggest the authors to group the trajectories according to dust and non dust days and also according to the levels of nitrogen and see which of these trajectories are passing over highly populated regions.

Reply: First of all, East Asia has three major dust aerosol sources: the western China sources, including the Taklimakan Desert and surrounding areas; the Mongolia sources, including the desert and semi-desert areas in southern Mongolia; and the northern China sources, including the BadainJaran Desert, the Tengger Desert, the Ulan Buh Desert and the Hunshandake Desert (Fig. SR1). Duolun and Zhurihe belong to the Hunshandake Desert in northern China. According to studies, 52%-71% of the dust storms that affect the Yellow Sea are from this sand source (Zhang and Gao, 2007; Gao et al., 2010). For our 14 dust samples, 13 events were from northern sources, and the remaining one was from northern sources but was transported to the northeast before being transported to the measurement site (the 72 h trajectory only showed transport from the northeast). Therefore, we collected sand samples at the Zhurihe site and used reported aerosol values from Duolun to characterize the aerosol particles in the source region. As the reviewer suggested, the coastal Yellow Sea region is affected by dust originating not only from the Duolun region but also from other regions. We added the nitrate and ammonium contents in sand samples collected from

other sand sources in China. We also added the reported concentrations of nitrate and ammonium in aerosol particles on dust days at or close to the dust source region in Table 5 in the revised manuscript. All these data verified that the mass concentrations of nitrate and ammonium relative to the total mass of sand particles were very low, i.e., less than $81\mu\text{g/g}$. We have added the modeling results of NO_x and NH_3 emissions using a 3-D air quality model and discussed the theoretical analysis of three categories in section 3.3 in the revised manuscript.

To characterize the transport paths of dust day samples more exactly, we reanalyzed the air mass trajectory of each sample at 1500 m altitude and redrew Fig. 5 to distinguish trajectories for samples collected on dust and non-dust days. According to the suggestion, we first we investigated whether these trajectories passed over highly populated regions. All trajectories involved transport from the source over highly populated regions and exhibited different transport times in these regions. We found that the concentrations of nitrate and ammonium depended on the transport distance over the sea, the mixed layer depth and the transport time over highly polluted regions. We have rewritten this section according to the suggestion to discuss the influence of transport paths on nitrate and ammonium contents in the revised manuscript.

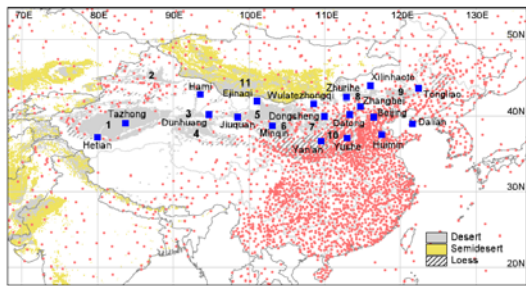


Figure SR1. Map of the main source regions of sand and dust storms in China (from Wang et al., 2008).

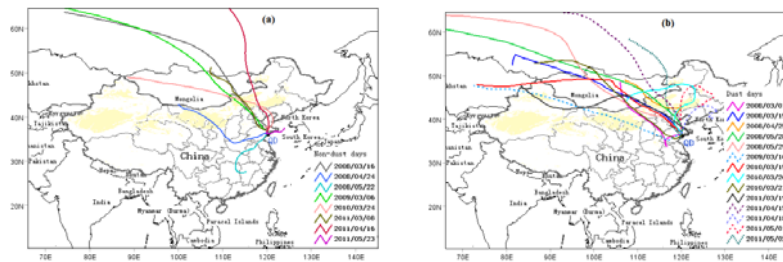


Figure 5. The 72-h backward trajectories for non-dust (a) and dust (b) samples from 2008 to 2011 (the yellow domains in the maps represent the dust source regions in China).

Table 5. Comparison of nitrate and ammonium content in sand and aerosol particles on dust days or close to the dust source region(unit: $\mu\text{g/g}$)

Sands sampled in dust source regions	Aerosols in or close to dust source region on dust days						
	Relative concentration ^a		Study region and data source	Relative concentration ^a		Aerosols in the coastal region of the Yellow Sea	
	NO_3^-	NH_4^+		NO_3^-	NH_4^+	NO_3^-	NH_4^+
Zhurihe (This study)	25.46±22.87	4.21±1.03	Duolun (Cui, 2009)	1200	900	Non-dust: 28,200±24,819	Non-dust: 24,063±21,515
AlxaLeft Banner, Inner Mongolia (NiuandZhang, 2000)	62.1±7.4	79.1±1.1	AlxaRightBanner, Inner Mongolia (NiuandZhang, 2000)	1975 ^b	4091 ^b	Category 1: 34,892±9570	Category 1: 22,571±7,016
Yanchi, Ningxia (NiuandZhang, 2000)	46.4±2.2	80.9±1.3	Hinterland of theTaklimakan Desert, Xinjiang (Dai et al., 2016)	142-233	2-15	Category 2: 5,542±5,117	Category 2: 4,758±5,698
			Average of SonidYouqi, Huade (Inner Mongolia), Zhangbei (Hebei) (Mori et al., 2003)	253	710	Category 3: 6,359±4,697	Category 3: 7,059±5,591
			Yulin, the north edge of Loess Plateau (Wang et al., 2011)	216.4	80.6		
			Golmud, Qinghai (Sheng et al., 2016)	892.9	- ^c		
			Hohhot, Inner Mongolia (Yang and Wang, 1995)	588.1	No data		

^aRelative concentration of nitrate and ammonium per aerosol particle mass

^bSamples collected on a floating dust day (Horizontal visibility less than 10000 m and very low wind speed)

^cThe ammonium concentration was lower than the detection limit of the analytical instrument.

Cui, W. L.: Chemical transformation of dust components and mixing mechanisms of dust with pollution aerosols during the long range transport from north to south China, M.S. thesis, Department of Environmental Science and Engineering, Fudan University, China, 38 pp., 2009.

Dai, Y. J.: Vertical distribution of characteristics of dust aerosols in the near-surface in hinterland of Taklimakan Desert, M.S. thesis,

- College of Resources and Environmental Science, Xinjiang University, China, 26 pp., 2016.
- Mori, I., Nishikawa, M., Tanimura, T., and Quan, H.: Change in size distribution and chemical composition of kosa (Asian dust) aerosol during long-range transport, *Atmos. Environ.*, 37, 4253-4263, 2003.
- Niu, S. J. and Zhang, C. C.: Researches on Sand Aerosol Chemical Composition and Enrichment Factor in the Spring at Helan Mountain Area, *Journal of Desert Research*, 20, 264-268, 2000.
- Sheng, Y., Yang, S., Han, Y., Zheng, Q., and Fang, X.: The concentrations and sources of nitrate in aerosol over Dolmud, Qinghai, China, *Journal of Desert Research*, 36, 792-797, 2016.
- Wang, Q. Z., Zhuang, G. S., Li, J., Huang, K., Zhang, R., Jiang, Y. L., Lin, Y. F., and Fu, J. S.: Mixing of dust with pollution on the transport path of Asian dust — Revealed from the aerosol over Yulin, the north edge of Loess Plateau, *Sci. Total. Environ.*, 409, 573-581, 2011.
- Yang, D. Z., Wang, C., Wen, Y. P., Yu, X. L., and Xiu, X. B.: Ananalysis of Two Sand Storms In Spring 1990, *Quarterly Journal of Applied Meteorology*, 6, 18-26, 1995.

Specific comments:

Q3. L11-13: Reconstruct the sentence.

Reply: These sentences have been rewritten as "Asian dust has been reported to transport anthropogenic reactive nitrogen from source areas to the oceans. In this study, we attempted to characterize the NH_4^+ and NO_3^- in atmospheric particles collected at a coastal site in northern China during spring dust events from 2008 to 2011."

Q4. L20-25: This is not conclusive from the discussions that follow. Statements like "storms were weak or slow moving" and "rapid transport in a strong dust storm" are not supported by proper analysis of the storm characteristics.

Reply: We have written the conclusion.

Q6. L35-36: This is contradicting L32-33.

Reply: We apologize for the confusion in the revision. We will revise the abstract sentence into "The dust deposition was an uncertain source of nitrogen for the ocean".

Q7. L40: These references point to anthropogenic contribution to atmospheric nitrogen deposition.

Reply: We apologize for the confusion in the revision. We have revised the abstract.

Q8. L62-64: The first part of the sentence seems to contradict the last part.

Reply: To avoid confusion, we have revised the sentence to "Although increased concentrations of NO_3^- and NH_4^+ in aerosol particles were observed on dust storm days in northern China relative to those non-dust days prior to the dust storm events, Zhang et al. (2010) also found that the concentrations of the two species were associated with the intensity of the dust storm, i.e., the stronger dust storms corresponded to the smaller increases. In other words, lower NO_3^- and NH_4^+ concentrations occurred during strong dust storm events than during weak dust events (Zhang et al., 2010)."

Q9. L79-81: Meaning is not clear.

Reply: We have deleted this sentence in the revised manuscript because this reference is not closely related to Asian dust.

Q10. L102: Zhurihe in Hunshandake Desert. Later you are using Duolun region which is not introduced in Section 2. It will be difficult for readers to follow if they are not very familiar with this region.

Reply: Thank you for the suggestion. The data at Duolun was adapted from the reference (Cui et al., 2009b). We have added the citation in the text of section 3.2. According to the former suggestion in Q2, we added new references for the dust components in source region to Table 4 in the revised manuscript (See reply to Q2). Additionally, we introduce Duolun and other study regions using references in Table 4.

Cui W. L.: Chemical transformation of dust components and mixing mechanisms of dust with pollution aerosols during the long range transport from north to south China, M.S. thesis, Department of Environmental Science and Engineering, Fudan University, 32-38 pp., 2009.

Q11. L135: Explain how the PMF model works.

Reply: We have added the PMF work principle in section 2.

Q12. L139: Explain how Williams' model works and cite the original paper.

Reply: We have added the work principle of the Williams' model and cited the original paper.

Q13. L140. Expand U10. In general, all the abbreviations used should be clearly defined.

Reply: We have added definitions for all the abbreviations in our revised manuscript.

Q14. L143: Meteorological data not "climatic" data.

Reply: The term "climatic" has been changed to "meteorological data".

Q15. L146: This heading does not reflect the text content.

Reply: The heading has been revised to "Other data sources and statistical analysis".

Q16. L152: Please provide details on the MICAPS information used.

Reply: We have supplemented the details on the MICAPS in section 2.1.

Q17. L164: What is the average TSP concentration on dust days?

Reply: We have added the average TSP concentration ($1140.3 \mu\text{g}\cdot\text{m}^{-3}$) on dust days in the revised manuscript.

Q18. L167: Please provide a brief description on how EF is calculated and what is the significance of using this method.

Reply: We have provided a brief description of EF and the significance of using EF in section 2.3.

Q19. L171-173: The authors were using MICAPS information of dust storm (which has to be explained) and now are relying on AI levels to define AD events. How are these two definitions consistent?

Reply: First, we defined dust days according to MICAPS information in Qingdao. However, the intensity of a dust event decreases gradually during the long-range transport, and high PM10 episodes of anthropogenic origin (dust is regarded as of natural origin) can be erroneously judged as a dust event in downwind regions. Hsu et al. (2008) proposed the “geometric mean $\times 2$ GSD” of AI concentrations in order to identify major Asian dust (AD) events in downwind regions and obtained good results. Our focus was the impact of long-range transported dust on aerosol samples in downwind area; therefore, we verified the long-range AD using reported GSD criterion in former manuscript. Just as discussed above, we have revised this section and replaced the AI criteria method using the model results in the revised manuscript.

Hsu, S. C., Liu, S. C., Huang, Y. T., Lung, S. C. C., Tsai, F., Tu, J. Y., and Kao, S. J.: A criterion for identifying Asian dust events based on AI concentration data collected from northern Taiwan between 2002 and early 2007, *Journal of Geophysical Research Atmospheres*, 113, 1044-1044, 2008.

Q20. L178-179: This has to be explained with respect to the EF of the anthropogenic elements.

Reply: We have added the calculation and significance of EF in section 2.3 in revised manuscript.

Q21. L214-216: You need to examine the dust sources, transport pathways (if passing over heavy populated regions), the height at which dust is transported together with dust concentration on a case by case basis to conclude these lines. This is very important for the entire paper. How do you decide “stronger a e “stronger a dust storm”?

Reply: Similar to the reply for Q2, we have revised the section according to the suggestion. In addition, the modeling dust concentration, and transport altitude were supplemented.

Q22. L225-230: The average for Case 1 is 700 $\mu\text{g}/\text{m}^3$ with values lying well above the average as is evident from Table 5. Again, there are TSP values in Case 2 in Table 5 which are lower than average of Case 1.

Reply: We have rewritten this section. By comparing the relative values of NH_4^+ and NO_3^- in dust day samples to those in comparison samples, the characteristics of dust day samples were discussed, and a theoretical analysis of the three categories was added.

Q23. L230-231: Again, what is your definition of “strong dust storm”? Without sufficient analysis I am not sure how “dust might be transported quickly” is factoring here. This

entire section has to be revisited.

Reply: According to the suggestion in Q2, we have added modeled dust concentrations over East Asia based on the CFORS model for dust event samples (<http://www-cfors.nies.go.jp/>) and rewritten the entire section considering whether trajectories passed over highly populated regions.

Q24. L242: How is the value 40.5 km/h arrived at? Is it estimated at the dust source region? How many dust storms were studied to derive this value? More explanation is needed.

Reply: According to Asian dust observations in China and Mongolia (He et al., 2008; Li et al., 2006; Natsagdorja et al., 2003; Zhan et al., 2009), we estimated an average wind speed threshold as 40.5 ± 9.9 km/h during dust storms. However, according to the suggestion in Q2, we have revised the entire section and discussed the influence of transport on the concentrations of nitrate and ammonium in dust day samples.

He, Q., Wei, W., Li, X., Ali, M., and Li, S.: Profile Characteristics of Wind Velocity, Temperature and Humidity in the Surface Layer during a Sandstorm Passing Taklimakan Desert Hinterland, *Desert and Oasis Meteorology*, 2, 6-11, 2008.

Li, N., Du, Z. X., Liu, Z. Y., Yang, H. J., Wu, J. D., and Lei, Y.: Change of wind speed and soil moisture during occurrence of dust storms, *Journal of Natural Disasters*, 15, 28-32, 2006.

Natsagdorj, L., Jugder, D., and Chung, Y. S.: Analysis of dust storms observed in Mongolia during 1937–1999, *Atmos. Environ.*, 37, 1401–1411, 2003.

Zhan, K. J., Zhao, M., Fang, E., Yang, Z. H., Zhang, Y. C., Guo, S. J., Zhang, J. C., Wang, Q. Q., and Wang, D. Z.: The wind speed characteristics of near-surface vertical gradient of 50m in sandstorm process in 2006, *Journal of Arid Land Resources & Environment*, 23, 100-105, 2009.

Q25. L250-252 needs explanation. Once the dust storms are properly categorized and the pathways are determined the interpretation of Table 5 might change

Reply: We have reanalyzed the trajectories and rewritten this section.

Q26. L250: Less than 40.5 km/h not 42.4 km/h.

Reply: We have revised this section.

Q27. L281-283: These statements need to be backed by more analysis of the dust events on a case by case basis.

Reply: We cannot discuss the contributions of dust to aerosols for each dust case because of the limited number of samples. The limited number of samples will result in an unrealistic source apportionment. Thus, we have rewritten this sentence.

Q28. L301-311: The text is very confusing. It is very difficult to follow when the authors are referring to TSP and when they are referring to IN or nitrate or ammonium.

Reply: We have rewritten these sentences. Additionally, we added the IN (now $N_{NH_4++NO_3^-}$ in revised manuscript) definition in section 3.6 and the flux of $N_{NH_4++NO_3^-}$ in Table 8 and revised several mistakes.

Table 8. Dry deposition of TSP ($\text{mg}/\text{m}^2/\text{month}$), particulate inorganic nitrogen ($\text{mg N}/\text{m}^2/\text{month}$) and some toxic trace metals ($\text{mg}/\text{m}^2/\text{month}$) on dust and non-dust days.

	Dry deposition flux							
	TSP	$\text{NO}_3^- \text{-N}$	$\text{NH}_4^+ \text{-N}$	$\text{N}_{\text{NH}_4^+ + \text{NO}_3^-}$	Fe	Cu	Pb	Zn
Category 1 ^a	8,000± 1800	65±9	24±14	90±17	533±179	2±0.3	0.3±0.3	6±2
Category 2 ^a	18000± 11,000	13±18	8±4	21±22	1300±100	3±2	0.08±0.04	4±1
Category 3 ^a	29,000± 31,000	26±6	17±8	42±12	2100±220	6±1	0.20±0.02	5±3
Non-dust	2,800± 700	48±33	15±8	63±39	190±110	1±1	0.09±0.1	5±4

^a The characterization of $\text{N}_{\text{NH}_4^+ + \text{NO}_3^-}$ concentration and sample information of the Category see in Table 3.

Technical corrections:

Q29. L260: Colors used in Figure 4 are not clear. Please indicate the dust source regions on the map.

Reply: We have redrawn Fig. 4 (now Fig. 5 in the revised version) to distinguish the trajectory of each sample collected on dust and non-dust days. The dust source regions in China are also now indicated in this figure.

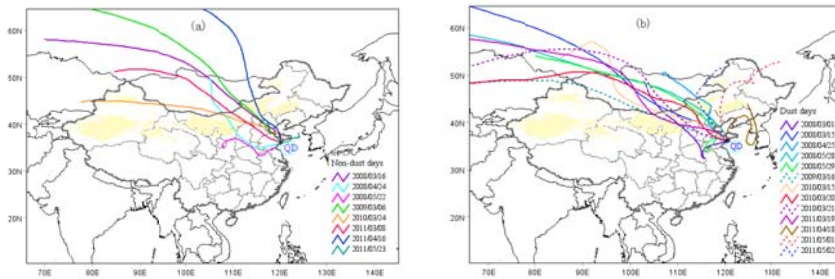


Figure 5. The 72-h backward trajectories for non-dust (a) and dust (b) samples from 2008 to 2011 (the yellow domains in the maps represent the dust source regions in China).

Q30. L343-442: Not proper attention has been given to the References and needs to be corrected.

Reply: We have updated and corrected the reference citations and format.

带格式的: 行距: 1.5 倍行距, 取消行号

1 **The concentration, source apportionment and deposition**
2 **flux of atmospheric particulate inorganic nitrogen in**
3 **atmospheric particles at a coastal site in the northern**
4 **China during dust events**

5 Jianhua Qi¹, Xiaohuan Liu¹, Xiaohong Yao¹, Ruifeng Zhang¹, Xiaojing Chen¹, Xuehui
6 Lin², Huiwang Gao¹, Ruhai Liu¹

7 ¹Key Laboratory of Marine Environment and Ecology, Ministry of Education, Ocean University of
8 China, Qingdao, 266100, China

9 ²Qingdao Institute of Marine Geology, Qingdao, 266100, China

10 Correspondence to: Jianhua Qi (qjianhua@ouc.edu.cn)

11
12 **Abstract.** Asian dust has been reported to carry anthropogenic reactive nitrogen during the transport
13 from its source areas to oceans. In this study, we attempted to characterize NH₄⁺ and NO₃⁻ in
14 atmospheric particles collected at a coastal site in northern China during spring dust events at a coastal
15 site in the northern China in every spring from 2008 to 2011. To understand the impacts of long-range
16 transport on particulate inorganic nitrogen associated with dust in downwind areas, aerosol samples were
17 collected in the Qingdao coastal region on dust and non-dust (ND) days in spring from 2008 to 2011.
18 The concentrations of water-soluble ions were measured by ion chromatography, with metal elements
19 detected using inductively coupled plasma atomic emission spectroscopy (ICP-AES) and inductively
20 coupled plasma-mass spectrometry (ICP-MS). Compared to atmospheric aerosols collected on ND days,
21 samples from dust days exhibited higher concentrations of particles and crustal elements. Total aerosol
22 particle concentrations increased by a factor of 5.9 on average dust days. On dust days, the average
23 concentrations of crustal elements (Se, Al, Fe, Ca and Mg) increased by over a factor of four relative to
24 those on ND days. Based on the mass concentrations of NH₄⁺ and NO₃⁻ in each total suspended particle
25 (TSP), the samples can be classified into two groups: in Category 1, the concentrations of NH₄⁺ and
26 NO₃⁻ were increased by a factor of 20%-440% on higher in some dust day samples relative to samples
27 collected immediately before or after dust event, while in Categories 2 and 3, these concentrations
28 decreased by 10-75% in other the dust day samples. For these two groups, NH₄⁺ in dust day samples

带格式的: 行距: 1.5 倍行距

带格式的: 字体: 小四, 上标
带格式的: 字体: 小四, 上标

带格式的: 字体: 非加粗
带格式的: 字体: 非加粗
带格式的: 字体: 非加粗
带格式的: 字体: 非加粗
带格式的: 字体: 非加粗
带格式的: 字体: 非加粗, 下标
带格式的: 字体: 非加粗, 上标
带格式的: 字体: 非加粗
带格式的: 字体: 非加粗, 下标
带格式的: 字体: 非加粗, 上标
带格式的: 字体: 非加粗
带格式的: 字体: 非加粗
带格式的: 字体: 非加粗

带格式的: 字体: 10 磅
带格式的: 字体: 10 磅
带格式的: 下标
带格式的: 上标
带格式的: 下标
带格式的: 上标
带格式的: 字体: 10 磅
带格式的: 字体: 10 磅

29 was present in the form of ammonium salts externally co-existing with dust aerosols or the residual of
30 incomplete reactions between ammonium salt and carbonate salts. The NO₃⁻ in the dust day samples
31 was attributed to interactions between anthropogenic air pollutants and dust particles during dust
32 transport from the source zone to the reception site. Back trajectory analysis showed that the
33 concentrations of NH₄⁺ and NO₃⁻ were apparently affected by the transport distance prior to the
34 reception site, the mixing layer depth and the residence time across highly polluted regions during
35 transport.

36 ~~The inorganic nitrogen content increased 1.2 to 9.2-fold during some dust events in which storms were~~
37 ~~weak or slow moving and reactions occurred during transport. By contrast, nitrate and ammonium~~
38 ~~exhibited very low concentrations (<20% of ND samples) or decreased concentrations in some cases as~~
39 ~~a result of the strong dilution effect of low nutrient dust particles arising from their rapid transport in a~~
40 ~~strong dust storm. If air masses traveled faster than 40.5±9.9 km/h, the inorganic nitrogen content of~~
41 ~~most aerosol samples decreased compared to that of ND samples because of the strong dilution effect.~~

42 ~~The concentration of atmospheric particulate inorganic nitrogen was related to not only the transport path~~
43 ~~and speed but also the local emissions and reaction conditions during transport. The positive matrix~~
44 ~~factorization (PMF) receptor model results showed that the contribution of soil dust dramatically~~
45 ~~increased from 23% to 36% (90% of the residuals < 3.0 and r² = 0.97) on dust days, with decreasing while~~
46 ~~the contributions of local anthropogenic sources decreased in inputs, especially that of secondary aerosols.~~

47 The dry deposition flux of atmospheric particulates increased from 2,800±700 mg/m²/month on
48 non-dust comparison ND days to 16,800±15,900 on dust days. The dry deposition flux of particulate
49 inorganic nitrogen increased by 1.19-285% to 5.8-fold under in Category 1 the weak dilution effects of
50 dust events. Relative to the comparison samples, The the average dry deposition flux of nitrate
51 decreased by 46%-73% by 46%-63% in Category 2, while that of ammonium decreased by 147% in
52 Category 3, or to ND levels when strong dilution occurred during dust events. The estimated dust
53 deposition flux varied greatly from event to event. Overall, a slight increase in dry deposition flux of
54 particulate inorganic nitrogen associated with dust events in this study relative to values in the literature
55 may reflect the combined effect of anthropogenic nitrogen emissions and the occurrence of natural dust
56 events. atmospheric input of nitrogen to the ocean was not enhanced by dust events, and dust deposition
57 was an uncertain source of nitrogen to the ocean.

带格式的：行距：1.5 倍行距

带格式的：字体：10 磅

带格式的：2 级，段落间距段前：
12 磅，段后：12 磅

带格式的：字体：10 磅

带格式的：字体：10 磅

带格式的：字体颜色：红色

带格式的：字体颜色：红色

58 Keywords: aerosols, nitrogen, dust, source apportionment, dry deposition flux

带格式的: 行距: 1.5 倍行距

59 1 Introduction

60 ~~Nitrogen is a key element for marine phytoplankton growth. Reactive~~ nitrogen carried in dust
61 particles can be transported ~~over a long distances, and the nitrogen deposition deposited to~~ in oceans has
62 been recognized as an important external source of ~~N~~nitrogen to supporting phytoplankton
63 ~~growth across vast distances at high wind speeds~~ (Duce et al., 2008; Zhang et al., 2010b). ~~Theis~~
64 ~~hypothesis has been evaluated in incubation experiments, and on-site in situ experiments, and through~~
65 ~~the use of satellite observational data. Additionally, bioavailable nutrients, via dust particle deposition,~~
66 ~~may enhance phytoplankton growth in some ocean areas~~ (Shi et al., 2012; Guo et al., 2012; Liu et al.,
67 2013; ~~Tan and Wang, 2014~~). ~~For example, Tan and Wang (2014) found that a phytoplankton bloom~~
68 ~~with a nearly four-fold increase in chlorophyll concentration occurred 10-13 days after dust deposition~~
69 ~~with an increase of chlorophyll concentrations increased by four-fold, and a phytoplankton bloom~~
70 ~~occurred 10-13 days after dust deposition. In addition, Banerjee and Kumar (2014) hypothesized~~
71 that dust-induced episodic phytoplankton blooms are important to the interannual variability of
72 chlorophyll in the Arabian Sea ~~away from active winter convection. Dramatic changes have occurred in~~
73 ~~the reactive nitrogen in anthropogenic emission in the last three decades, e.g., large increases in NH₃~~
74 ~~and NO_x in emissions in China and other developing countries in Asia and a substantial decrease in~~
75 ~~emissions in Europe (Grice et al., 2009; Liu et al., 2017; Ohara et al., 2007; Skjoth and Hertel, 2013).~~
76 ~~These changes may greatly affect the nitrogen carried by dust particles, but few recent studies have~~
77 ~~examined this issue.~~

78 Asian dust ~~is~~ one of the main components of dust worldwide, ~~affects northern China and the eastern~~
79 ~~area of the China Sea.~~ Asian dust has been reported to cross over the mainland and the marginal seas of
80 ~~China and reach as far as the remote~~ can also affect the northern Pacific Ocean (Zhang and Gao, 2007;
81 ~~Tan and Wang, 2014~~) via long range transport by west winds. During the long-range transport, ~~the~~ dust
82 ~~storm~~ particles may continually mix with anthropogenic gas and particles, ~~and consequently~~
83 ~~occurring resulting in complicated chemical reactions~~ (Cui et al., 2009; Wang et al., 2011; Wang
84 et al., 2015; Wang et al., 2017). However, the extent of these chemical reactions varies widely and
85 depends on the meteorological conditions, such as cloud fraction, wind speed, relative humidity and

86 atmospheric circulation (Yang et al., 2002; Li et al., 2014; Ma et al., 2012) from local sources along
87 the pathway to carry desert dust and anthropogenic aerosols to downwind areas. The physical and
88 chemical characteristics of atmospheric particulates downwind of dust weather are remarkably different
89 from those normally present (Yang et al., 2002; Li et al., 2014; Ma et al., 2012). Additionally, the
90 concentrations and characteristics of atmospheric particulate inorganic nitrogen species in downwind
91 areas are greatly affected by dust weather.

92 For example, a few studies have shown that Some researchers have found that inorganic nitrogen
93 species in aerosols have high concentrations during Asian dust events. The concentrations of
94 atmospheric particulate NO_3^- and NH_4^+ on dust storm days were 2-5 times higher larger than those on
95 those non-dust storm (ND) days prior to the events in Beijing (Liu et al., 2014; Liu and Bei, 2016). Xu
96 et al. (2014) also reported found that concentrations of particulate SO_4^{2-} and NO_3^- were simultaneously
97 increased in during dust storm events on in along the northern boundary of the Tibetan Plateau because
98 of the enriched dust including more acidic species or anthropogenic aerosols. Compared to those on
99 ND days, higher concentrations of NO_3^- and NH_4^+ in aerosol particles were observed on dust storm
100 days in northern China, and NO_3^- and NH_4^+ showed lower concentrations during strong dust storm
101 events than during weak dust events (Zhang et al., 2010). Fitzgerald et al. (2015) found that almost
102 nearly all Asian dust observed in Korea contains contained considerable amounts of nitrate and
103 proposed that because pollution plumes mix with dust the dust from the Gobi and Taklamakan Deserts
104 probably mixed and reacted with anthropogenic air pollutants during the transport and are transported
105 over the Asian continent. Although increased concentrations of NO_3^- and NH_4^+ in aerosol particles were
106 observed on dust storm days in the northern China relative to Compared to those on Nd non-dust days
107 prior to the dust storm events.

108 Zhang et al. (2010a) also found that the concentrations of the two species were associated with the
109 intensity of the dust storm, i.e., the stronger dust storms corresponded to the smaller increases. In other
110 words, lower NO_3^- and NH_4^+ concentrations occurred during strong dust storm events than during weak
111 dust events (Zhang et al., 2010a).

112 higher concentrations of NO_3^- and NH_4^+ in aerosol particles were observed on dust storm days in
113 northern China, and NO_3^- and NH_4^+ showed lower concentrations during strong dust storm events than
114 during weak dust events (Zhang et al., 2010).

115 On the other hand, However, some studies reported reported observed that the reverse result the

116 concentrations of inorganic nitrogen in aerosols decreased on dust storm days. For ~~example~~example,
117 ~~at~~At Yulin, a rural site near the Asian dust source region, the concentration of NO_3^- ~~in atmospheric~~
118 ~~aerosols on dust days was~~ significantly ~~significantly lower in comparison to the concentration~~
119 ~~measured immediately before or after the event, as a result of the dilution effect~~decreased, ~~in~~
120 ~~comaprison to the~~ measured immediately before or after the event, in aerosols on dust days (Wang
121 et al., 2016). ~~Even in Shanghai, a mega city being located at a few thousands~~ kilometerskilometers from
122 ~~dust source zones in China, t~~he absolute abundanees concentrations of NO_3^- and NH_4^+ were notably
123 lower in ~~the~~ ~~oberved~~observed dust plumes than in a polluted air parcel ~~immediately~~ ~~oberved~~ prior to the
124 ~~dust events (Wang et al., 2013). because dust plumes are often separated by the arrival of a cold front in~~
125 ~~Shanghai, China (Wang et al., 2013).~~ Li et al. (2014) ~~also~~ found that the concentrations of nitrate and
126 ammonium ~~in downwind aerosol particles~~ were decreased on dust storm days ~~together~~, with a decreasing
127 ratio of ~~the total~~ soluble inorganic ions to $\text{PM}_{2.5}$ in the Yellow River Delta, China. When dust ~~is was~~
128 rapidly transported from desert regions without passing through ~~a~~ major urban areas and ~~lingers~~
129 ~~lingering~~ over the Yellow Sea, the concentrations and size distributions of nitrate and ammonium ~~have~~
130 ~~had~~ no significant variation in heavy Asian dust (AD) plumes (Kang et al., 2013). ~~Nitrate and~~
131 ~~ammonium also exhibited different concentration variations in other desert regions. Jaafar et al. (2014)~~
132 ~~found that nitrate was more abundant than ammonium, which showed no concentration variation in~~
133 ~~non dust aerosol particles during dust episodes originating from both the African and Arabian deserts.~~
134 ~~The contradictory results highlight the importance of investigating the concentrations of ammonium~~
135 ~~and nitrate in atmospheric particles during dust events based on a larger database.~~ ~~In this study, a~~ffect
136 of dust events on the inorganic nitrogen concentration in downwind aerosols is complicated because it
137 involves many factors, such as the mixing state and transport pathway. The effect of AD as a nitrogen
138 source on biogeochemical cycles and marine ecology is not adequately understood. Understanding the
139 variations in the concentration and deposition flux of atmospheric particulate nitrogen on dust days is
140 essential to quantifying the impacts of nutrients on the marine environment and primary production.
141 ~~To understand the influence of dust on atmospheric nitrogen,~~ we collected ~~atmospheric~~ aerosol samples
142 ~~particles during and prior to (or~~ ~~post~~after, when no sample was collected prior to) dust events from ~~at a~~
143 ~~coastal site in the promixty~~adjacent to the coastal region of the Yellow Sea ~~in~~ during the ~~every~~ spring
144 from 2008 to 2011; when ~~a smaller~~ outbreak peak there is a high frequency of dust storms occurred;
145 ~~from 2008 to 2011. Then,~~ ~~w~~e measured ~~analyzed~~ concentrations of the inorganic nitrogen

带格式的：非突出显示

带格式的：非突出显示

带格式的：非突出显示

146 concentrations in the aerosol samples as well as other components for facilitating analysis. We first
147 characterized the concentrations of inorganic nitrogen concentrations in various dust events
148 relative to the concentrations in samples collected either prior to or after the events. We then conducted
149 source apportionment to quantify their sources. Finally, we calculated and deposition flux of
150 atmospheric particulate inorganic nitrogen in during dust events and compared the results with the
151 values in the literature in order to update the flux values due to dynamic changes in anthropogenic
152 emissions and other factors.

153 2 Experimental Materials and methods

154 2.1 Sampling

155 ~~As shown in Fig. 1 shows the sampling site, which is situated at the top of a coastal hill (Baguanshan)~~
156 ~~in Qingdao in northern China (36° 6' N, 120° 19' E, 77 m above sea level) and is approximately 1.0 km~~
157 ~~from the Yellow Sea to the east. A high-volume air sampler (Model KC-1000, Qingdao Laoshan~~
158 ~~Electronic Instrument Complex Co., Ltd.) was set up on the roof of an two-story office building to~~
159 ~~collect total suspended particle (TSP) samples on quartz microfiber filters. ~~showed the sampling site,~~~~
160 ~~which is situated at the top of a coastal hill (Baguanshan) in the northern China (36° 6' N, 120° 19' E, 77~~
161 ~~m above sea level) and approximately 1.0 km from the Yellow Sea in the east. total suspended particles~~
162 ~~(TSP) were collected at the Baguanshan site in the coastal region of the Yellow Sea. The samples were~~
163 ~~collected with quartz microfiber filters (Whatman QM-A) at a flow rate of 1 m³/min. Prior to the~~
164 ~~sampling, the filters were heated at 450°C for 4.5 h to remove organic compounds. Our sample~~
165 ~~collection strategy involved collecting dust samples representing long-range transported particles. We~~
166 ~~followed the definition of dust events adopted in the regulations of surface meteorological observations~~
167 ~~of China (CMA, 2004; Wang et al., 2008) and identified dust events based on the meteorological~~
168 ~~records (Weather Phenomenon) of Qingdao from Meteorological Information Comprehensive Analysis~~
169 ~~and Process System (MICAPS) of the China Meteorological Administration. Each dust sample was~~
170 ~~collected over 4 hrs. and the sampling started only when the PM₁₀ and dust mass concentration available~~
171 ~~on the website (<http://www-cfors.nies.go.jp/~cfors/>; <http://www.qepb.gov.cn/m2/>) had increased greatly.~~
172 ~~This approach made the dust sample more representative relative to urban background. For dust events~~
173 ~~with durations of less than one day, only one sample was collected. For dust events with~~
174 ~~durations greater than one day, a 4-hr dust sample was collected once per day. Table 1 lists the sampling~~
175 ~~information. Based on the forecast, we also collected aerosol particle samples immediately before~~
176 ~~or after the dust event for comparison. These comparison samples were further classified into sunny day~~
177 ~~samples, cloudy day samples and post-dust samples. The post-dust samples were collected under clear~~
178 ~~and sunny weather conditions and low PM₁₀ mass concentrations.~~

179 ~~using a high volume air sampler (Model KC-1000, Qingdao Laoshan Electronic Instrument Complex~~
180 ~~Co., Ltd.) with a flow rate of 1 m³/min was set up on the roof of an two-story office~~
181 ~~building for collecting total suspended particles (TSP) on quartz microfiber filters (Whatman QM-A) with~~

带格式的：行距：1.5 倍行距

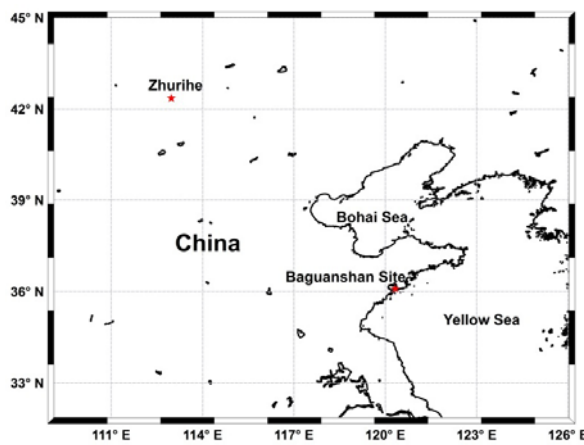
182 ~~a flow rate of 1 m³/min (36° 6' N, 120° 19' E, 77 m above sea level) approximately 1.0 km from the~~
183 ~~shore. Prior to the sampling, the filters were heated at 450°C for 4.5 h to remove organic~~
184 ~~compounds. Moreover, the concentration of Al referring to the total Al concentration in TSP samples~~
185 ~~were used to confirm the division of dust or comparison samples according to the criterion~~
186 ~~"geometric mean×2GSD" proposed by Hsu et al. (2008).~~

187

188 ~~Since Asian dust events at the sampling site mostly occur in the spring, we collected samples~~
189 ~~during every spring, i.e., from March to May, from 2008-2011. A smaller peak in Asian dust was observed~~
190 ~~in eastern China in 2008-2011, which followed a larger peak in 2000-2003 during this century (Fig.~~
191 ~~6). Overall, a total of 14 sets of dust samples and 8 sets of comparison samples were collected for this~~
192 ~~study.~~

193 ~~To facilitate the coastal sampling data analysis, the sand samples were collected at the Zhurihe site~~
194 ~~(42°22'N, 112°58'E) in the Hunshandake Desert, one of the main Chinese sand deserts, in April 2012. After~~
195 ~~the sand samples were packed in clean plastic sample bags, the samples and were stored below -20°C~~
196 ~~before the transfer. An ice-box was used to store the samples which were during transported to the lab~~
197 ~~for chemical analysis.~~

198



199

200 **Figure 1.** Location of the aerosol and dust sampling site.

201 2.2 Analysis

202 The aerosol samples were ~~allowed to achieve equilibrium in a air-conditioned chamber at a constant~~
203 ~~relative humidity and temperature for 24hrs. balanced in a air-condition relative humidity and~~
204 ~~temperature-controlled chamber at a constant relative humidity and temperature for 24 hrs until the~~
205 ~~particle before weights remained constanting. The mass concentrations of TSP were calculated~~

带格式的：字体：(默认) +中文正文

带格式的：行距：1.5 倍行距

206 according to the particle masses and the sampling volume. The sample membranes were then cut into
207 several portions for analysis.

208 One portion of each aerosol sample and 0.1 g of parallel sand sample were ultrasonically
209 extracted with ultra-pure water in an ice water bath, and the concentration of inorganic water-soluble
210 ions was determined via using ICS-3000 ion chromatography (Qi et al., 2011). The parallel sand
211 samples collected at the Zhurihe site from the Hunshandake Desert were analyzed using the same
212 procedure. We refer to dissolved inorganic nitrogen (DIN), the sum of nitrate and ammonium, in the
213 later discussion due to the very low concentration of nitrite in the samples.

214
215 One portion of each aerosol filter was cut into 60 cm² pieces and digested with HNO₃+HClO₄+HF
216 (5:2:2 in volume) at 160°C using an electric heating plate. A blank membrane was also analyzed using
217 the same procedure to ensure analytical precision. Cu, Zn, Cr, Sc and Pb were measured by using an
218 inductively coupled plasma-mass spectrometry (Thermo X Series 2), while Al, Ca, Fe, Na and Mg were
219 detected by using an inductively coupled plasma-atomic emission spectroscopy (IRIS Intrepid II XSP).
220 The membrane blanks have been corrected for in the calculation of the. The membrane blanks have
221 been deducted to calculate the metal concentrations were determined by calibrating the measured
222 concentrations of samples using m for analysis below membrane blanks.

223 **Table 1.** Detection limits, precisions and recoveries of water-soluble ions and metal elements.

Component	Measurement method	Detection limit (μg·L ⁻¹)	Precision (RSD%)	Recovery (%)
NO ₃ ⁻	IC	2.72	1.54	97
SO ₄ ²⁻		1.62	1.55	98
NH ₄ ⁺		0.4	1.10	97
Ca ²⁺		0.44	0.79	94
Cu	ICP-MS (Xin et al., 2012)	0.006	4.0	106
Zn		0.009	2.5	102
Cr		0.004	3.0	95
Se		0.002	2.4	97
Pb		0.008	3.9	104

带格式的: 行距: 1.5 倍行距

带格式的: 字体: (默认) Times New Roman, 10 磅

带格式的: 行距: 1.5 倍行距

带格式的: 行距: 1.5 倍行距

带格式的: 行距: 1.5 倍行距

带格式的: 行距: 1.5 倍行距

带格式的: 行距: 1.5 倍行距

带格式的: 行距: 1.5 倍行距

带格式的: 行距: 1.5 倍行距

带格式的: 行距: 1.5 倍行距

带格式的: 行距: 1.5 倍行距

带格式的: 行距: 1.5 倍行距

Al	ICP-AES (Lin et al., 1998)	7.9	0.6	103
Ca		5.0	1.2	99
Fe		2.6	0.7	104
Na		3.0	0.6	99
Mg		0.6	0.6	105
Hg	CVAFS	0.0001	6.6	105
As	CVAFS	0.1	5.0	98

带格式的: 行距: 1.5 倍行距

带格式的: 行距: 1.5 倍行距

带格式的: 行距: 1.5 倍行距

带格式的: 行距: 1.5 倍行距

带格式的: 行距: 1.5 倍行距

带格式的: 行距: 1.5 倍行距

带格式的: 行距: 1.5 倍行距

224 One portion of each aerosol sample was digested by adding with HNO₃ solution (10% HNO₃, 1.6 M)
 225 at 160°C for 20 min in a microwave digestion system (CEM, U.S.). Hg and As in sample extracts were
 226 analyzed following the U.S. Environmental Protection Agency method 1631E (U.S. EPA, 2002) using
 227 cold vapor atomic fluorescence spectrometry (CVAFS).

228 The detection limits, precisions and recoveries of water-soluble ions and metal elements are listed in
 229 Table 42.

230 2.3 Computational modeling

231 The enrichment factor of metal elements was given by

$$232 \text{EF}_i = \frac{(X_i/X_{\text{Re}})_{\text{aerosols}}}{(X_i/X_{\text{Re}})_{\text{crust}}} \quad (1)$$

带格式的: 行距: 1.5 倍行距

域代码已更改

带格式的: 字体: (默认) Times New Roman

233 where subscripts i and Re refer to the studied metal and the reference metal; (X_i/X_{Re})_{aerosols}
 234 is the concentration ratio of metal i to metal Re in the aerosol samples; and (X_i/X_{Re})_{crust} is the
 235 ratio of metal i to metal Re in the Earth crust. For the calculation of the enrichment factor of the
 236 metal elements, scandium was used as the reference element (Han et al., 2012), and the abundance
 237 of elements in the Earth's crust given by Taylor (1964) was adopted.

238 To determine the origins of sampled air masses, the 72 h air mass back trajectories were calculated
 239 for each TSP sample using TrajStat software (Wang et al., 2009) and the NOAA GDAS archive data
 240 ([http:// www.arl.noaa.gov/ready/hysplit4.html](http://www.arl.noaa.gov/ready/hysplit4.html)). The air mass back trajectories were calculated at an
 241 altitude of 10500 m to identify the dust origin.

242 The positive matrix factorization (PMF) is a commonly used receptor modeling method. This model
 243 can quantify the contribution of sources to samples based on the composition or fingerprints of the
 244 sources (Paatero and Tapper, 1993; Paatero, 1997). The measured composition data can be represented

带格式的: 字体: 10 磅

带格式的: 行距: 1.5 倍行距

245 by a matrix X of i by j dimensions, in which i number of samples and j chemical species were
246 measured, with uncertainty. X can be factorized as a source profile matrix (F) with the number of
247 source factors (p) and a contribution matrix (G) of each source factor to each individual sample, as
248 shown in Equation 2, receptor modeling method (Paatero and Tapper, 1993; Paatero, 1997).

$$249 X_{ij} = \sum_{k=1}^p G_{jk} F_{ki} + E_{ij} \quad (2)$$

250 where E_{ij} is the residual for species j of the i -th sample.

251 The aim of the model is to minimize a objective function Q , which was calculated from the residual
252 and uncertainty of all samples (Equation 3), to obtain the most optimal factor contributions and

$$253 profiles, $Q = \sum_{i=1}^n \sum_{j=1}^m (E_{ij}/U_{ij})^2$ (3)$$

254 EPA PMF 3.0 model was used to obtain the source apportionment of atmospheric particulates on
255 dust and comparison days. The correlation coefficient between the predicted and observed
256 concentrations was 0.97.

257
258 Dry deposition velocities were obtained using Williams' model (Williams, 1982) and by accounting
259 for particle growth (Qi et al., 2005). Williams' model is a two-layer model to calculate the dry velocity
260 of size-segregated particle over the water. At upper layer below a reference height (10 m), the
261 deposition of aerosols particles is governed by turbulent transfer and gravitational settling. In the
262 deposition layer, gravitational settling of particles is affected by particle growth due to high relative
263 humidity. To obtain the deposition velocity of different particle size, Williams' model need many input
264 parameters, such as the wind speed at 10m height (U_{10}), air/water temperature, relative humidity,
265 Relative humidity, air temperature and U_{10} obtained from the National Centers for Environmental
266 Prediction (NCEP) were used in the model as the meteorological inputs this study. Surface seawater
267 temperature was collected from the European Centre for Medium-Range Weather Forecasts
268 (ECMWF). The meteorological data and seawater temperature data had a six-hour resolution.
269 According to a previously reported method (Qi et al., 2013), the dry deposition fluxes of the particles
270 and the nitrogen species were calculated for dust and comparison days.

271 The CMAQ model (v5.0.2) was applied over the East Asia area to simulate the concentrations of
272 PM₁₀, NO_x and NH₃ for 14 samples collected during 11 dust events. The simulated domain contains
273 164×97 grid cells with a 36 km spatial resolution. The vertical resolution includes 14 layers from
274 surface to tropopause, with the first model layer height of 36m above the ground level. The

带格式的 ... [1]

带格式的 ... [2]

带格式的 ... [3]

带格式的: 字体: 10 磅

带格式的: 缩进: 首行缩进: 1 字符

带格式的 ... [4]

带格式的: 字体: 10 磅

带格式的: 缩进: 首行缩进: 1 字符

带格式的 ... [5]

275 meteorological fields were generated by the Weather Research and Forecasting (WRF) Model (v3.7).
276 Considering that the simulated area is connected to the Yellow Sea, the CB05Cl chemical mechanism
277 was chosen to simulate the gas-phase chemistry. The emissions of NOX and NH3over East Asia for
278 each dust event were also modeled using the CMAQ model according to the emission inventory in
279 2008, which was generated by extrapolating the 2006 activity data to the year 2008 using the method
280 described by Zhang et al.(2009). Initial conditions (ICONS)and boundary conditions were generated
281 from a global chemistry model of GEOS-CHEM. All the dust events simulations are performed
282 separately, each with a 1-week spin-up period to minimize the influence of the ICONs. Validation of
283 the application of the CMAQ model in China has been reported by Liu et al. (2010a, b). The spatial
284 distribution of PM10 concentrations for each dust event was consistent with the model results of dust
285 by the Chemical Weather Forecast System (CFORS) by Uno et al. (2003).~~he Chemical Weather~~
286 ~~Forecast SystemCFORS.~~

带格式的: 字体: (默认) Times
New Roman, 10 磅

带格式的: 字体: +西文正文, 10
磅

带格式的: 行距: 1.5 倍行距

287 **2.4 ~~Statistical analysis~~Other data sources and Statistical analysis**

288 Meteorological data were obtained from the Qingdao Meteorological Administration
289 (<http://qdqx.qingdao.gov.cn/zdz/ystj.aspx>) and the ~~Meteorological Information Comprehensive~~
290 ~~Analysis and Process System (MICAPS)~~ of the Meteorological Administration of China. ~~NO₂ and air~~
291 ~~quality index (AQI) data were downloaded from the Qingdao Environmental Protection Bureau~~
292 (~~<http://www.qepb.gov.cn/m2/>~~). Different weather characteristics, such as sunny days, cloudy days and
293 dust days, were defined according to ~~information of MICAPS information and Qingdao Meteorological~~
294 ~~Administration. The Meteorological Information Comprehensive Analysis and Process System~~
295 ~~(MICAPS).~~ ~~he Chemical Weather Forecast SystemCFORS.~~

带格式的: 字体: (默认) Times
New Roman, 10 磅

带格式的: 字体: 10 磅

296 According to the altitude, longitude and latitude of the 72 h air mass back trajectory of each dust
297 sample, the pressure level, temperature and relative humidity data along the path of the air mass were
298 derived from the NCEP/NCAR re-analysis system
299 (<http://www.esrl.noaa.gov/psd/data/gridded/data.ncep.reanalysis.html>) for each sample. The mixed
300 layer depth during the air mass transport of dust samples was obtained from the HYSPLIT Trajectory
301 Model (<http://ready.arl.noaa.gov/hypub-bin/trajsrc.pl>) using the same method. Spearman correlation
302 analysis was applied to examine the relationships of nitrate and ammonium with transport parameters.
303 and P values of <0.05 were considered to be statistically significant.

304 **3 Results and discussion**

305 **3.1 Characterization of aerosol samples collected during dust events**

306 To support our analysis, the dust intensity and influence range of the dust events modeled by Uno et al.
307 (2003) were analyzed, and the spatial distributions of dust concentration over East Asia during each dust
308 sampling day are shown in Fig. 2 and Fig. S3. Almost all dust events originated in northern or
309 northwestern China and passed over the sampling site. However, Sample 20110415 was judged to
310 be local blowing dust because no corresponding high dust concentrations were observed in the dust
311 source areas; this sample was therefore excluded from further analysis.

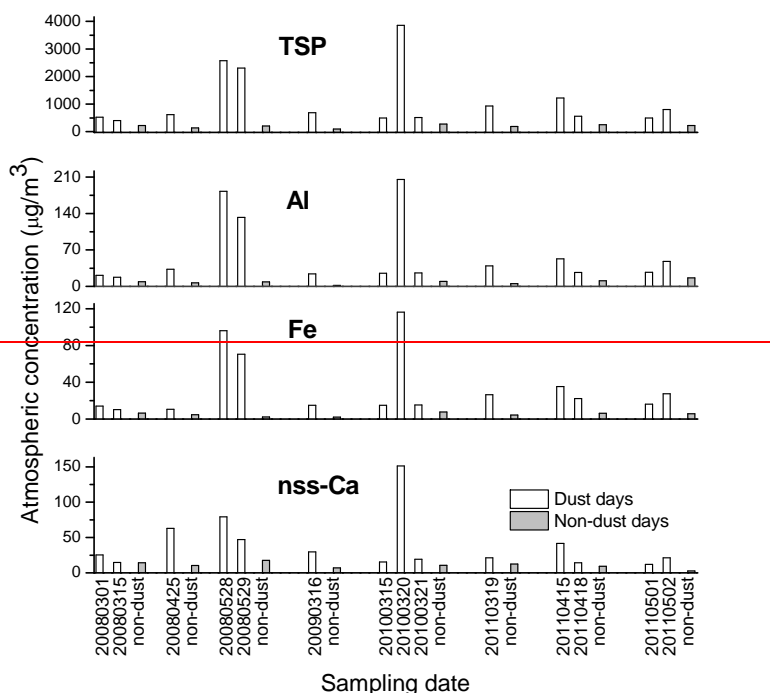
带格式的：行距：1.5 倍行距

带格式的：两端对齐，缩进：首行缩进：1 字符，定义网格后自动调整右缩进，段落间距段前：0.5 行

带格式的：字体：10 磅

带格式的：行距：1.5 倍行距

带格式的：字体：五号，非加粗，字体颜色：黑色



315 **Figure 23.** Concentrations of TSP, Al, Fe and nss-Ca in aerosol samples collected in the coastal region of the
316 Yellow Sea on non-dust and dust days from 2008 to 2011.

带格式的：行距：1.5 倍行距

318 Before characterizing the inorganic To understand the impact of dust events on atmospheric
319 particulate nitrogen in atmospheric particles at Baguanshan site, downwind areas, we collected aerosol
320 samples in the coastal region of the Yellow Sea in the spring from 2008 to 2011. We first examined

321 the mass concentrations of particles-TSP and as well as concentrations of crustal and anthropogenic
322 metals to compare samples collected on dust days and immediately before or after days. in aerosol
323 samples. Although metal concentrations in aerosols collected on different dust days varied, some
324 characterizations The comparative results are highlighted below. The concentration of atmospheric
325 particulate increased on dust days. On non-dust (ND) days For these comparison samples, aerosol
326 particles the TSP concentrations varied in the range of from 94 to 275 $\mu\text{g}\cdot\text{m}^{-3}$, with an average of 201
327 $\mu\text{g}\cdot\text{m}^{-3}$ (Fig. 2). The TSP mass concentration Particle concentrations were increased substantially
328 increased to 501-3857 $\mu\text{g}\cdot\text{m}^{-3}$ on in dust day samples, with an average of 1140.2 $\mu\text{g}\cdot\text{m}^{-3}$. In each dust
329 day-comparison day sample pair, the mass concentration of The-TSPs increased by concentration on
330 dust days was 1.80-14.01303% with the median value of 537% (mean: 5.9) higher than that on ND
331 days. The A similar increase was present in the crustal elements increased considerably with the
332 increasing particle concentrations when dust events occurred in each pair of samples. For example, the
333 mean concentrations of Sc, Al, Fe, Ca and Mg were increased by over a factor of four in dust day
334 samples relative to the comparison samples. In addition, As shown in Table 2, the enrichment factors
335 (EF) of Al, Fe, Ca, and Mg were less than three in dust day samples but lower less than ten 14 on ND
336 days in comparison samples and decreased to less than three on dust days in each pair (Table 3). These
337 lower data values are indicative of these elements from the the primarily crustal origins of these
338 elements. We found that the mean concentrations of Se, Al, Fe, Ca and Mg increased by over a factor of
339 four as compared to those on ND days. Al concentrations in dust weather increased 1.7 to 21.9-fold
340 (mean: 6.9) on ND days. The Al concentration of the “geometric mean $\times 2\text{GSD}$ ” (where GSD is the
341 geometric standard deviation) was used as a criterion to define major AD events in areas of East Asia
342 (Hsu et al., 2008). Al concentrations were higher than the criterion level in all dust samples, which
343 indicated that the samples we collected on dust days were truly affected by dust events. Fe was 10.3
344 times higher on dust days than on ND days. Additionally, nss-Ca, a typical dust index, increased
345 3.6-fold on dust days (Fig. 2). The EF of the anthropogenic metal elements decreased on dust days. Cu,
346 Pb, Zn, Cr, Hg and As had high EFs, much greater than 10, on ND days, which indicated that these metal
347 elements were mainly from anthropogenic sources. Although The the average mass concentrations of
348 these anthropogenic elements such as Cu, Pb, Zn, Cr, Hg and As on in dust day sample increased
349 1-107% to 7.2-fold 22% on average relative compared to those in comparison samples, the EF of the
350 anthropogenic metal elements decreased in the dust day samples on ND days. Additionally, the EFs of

351 ~~these anthropogenic elements decreased on dust days. These data are consistent with the very low EFs~~
 352 ~~of these elements in dust particles. Thus This pattern, indicated a decreasing relative contribution of~~
 353 ~~the influence of anthropogenic sources on atmospheric particulates decreased to the total TSP mass on~~
 354 ~~in dust day samples.~~

355

356 **Table 2.** The average concentrations and EFs of metal elements on dust and non-dust days.

Element	Concentration (ng/m ³)		EF*	
	Non-dust days	Dust days	Non-dust days	Dust days
Se	4.44	43.90	-	-
Al	8.53×10 ³	6.86×10 ⁴	3.8	4.4
Fe	4.91×10 ³	3.88×10 ⁴	3.	4.2
Ca	4.05×10 ⁴	4.29×10 ⁴	14.0	2.1
Mg	4.62×10 ³	4.58×10 ⁴	3.5	4.1
Cu	50.2	124.5	36.3	6.1
Pb	127.9	221.0	389.4	56.1
Zn	340.0	457.7	248.9	20.6
Cr	33.8	244.0	44.0	11.1
Hg	0.26	0.36	176.0	13.8
As	25.5	27.4	707.2	43.9

357 *The EF factor was calculated using Scandium as the reference element (Han et al., 2010).

358 **3.2 Concentration ~~distribution~~ of inorganic nitrogen in dust ~~events~~ day samples**

359 ~~As discussed above, the concentrations of TSP and metal elements increased on dust days~~
 360 ~~compared to those on ND days. However, When the mass concentrations of inorganic nitrogen species~~
 361 ~~NH₄⁺ and NO₃⁻ in each pair of TSP samples were compared, exhibited different variations in particles~~
 362 ~~and crustal metal elements. The concentrations of ammonium-NH₄⁺ increased by a factor of~~
 363 ~~1.220%-5.747% in some dust day samples (20080301, 20080315, 20090316, 20100315, 20100320,~~
 364 ~~20100315, 20110415 and 20110418), but slightly or greatly and decreased by 40-85% or had a very low~~

带格式的: 行距: 1.5 倍行距

带格式的: 行距: 1.5 倍行距

带格式的: 行距: 1.5 倍行距

带格式的: 行距: 1.5 倍行距

带格式的: 行距: 1.5 倍行距

带格式的: 行距: 1.5 倍行距

带格式的: 行距: 1.5 倍行距

带格式的: 行距: 1.5 倍行距

带格式的: 行距: 1.5 倍行距

带格式的: 行距: 1.5 倍行距

带格式的: 行距: 1.5 倍行距

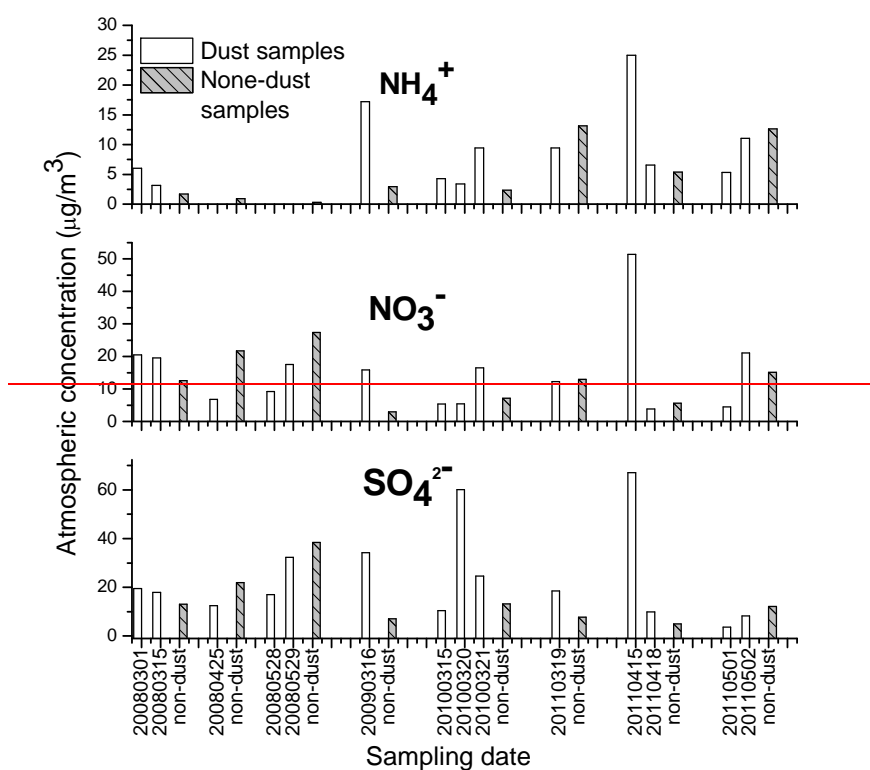
带格式的: 行距: 1.5 倍行距

带格式的: 行距: 1.5 倍行距

带格式的: 下标

带格式的: 上标

365 concentration (less than 20% of that on ND days) in other dust day samples (Fig. 3, Table S2). The
 366 same was general true for the measured concentration of NO_3^- . Similar to ammonium, nitrate displayed
 367 two different concentration variations on dust days. Nitrate concentrations increased by a factor of
 368 1.4–9.2 on some dust days and decreased on other dust days. The secondary inorganic ion SO_4^{2-} exhibited
 369 concentration variations that were similar to those of nitrate. Therefore, the influence of dust on these
 370 secondary ions was different from that on crustal metal elements, and the effect of dust on inorganic
 371 nitrogen differed during different types of dust events.



372
 373 **Figure 34. Mass concentration of NH_4^+ , NO_3^- and SO_4^{2-} in aerosol samples collected at the Baguanshan site**
 374 **on dust and comparison days during March–May in the coastal region of the Yellow Sea on non-dust and dust**
 375 **days from 2008 to 2011.**
 376 Considering the relative values of NH_4^+ and NO_3^- in dust day samples relative to comparison samples,
 377 the dust day samples can be classified into three categories (Table 4). In Category 1, the mass
 378 concentrations of NH_4^+ and NO_3^- were larger in dust day sample than in the comparison samples. In

带格式的：下标

带格式的：上标

带格式的：行距：1.5 倍行距

379 Category 2, the reverse was true. In Category 3, the mass concentrations of NO₃⁻ were lower in the dust
380 samples than in the comparison samples, whereas the reverse was true for NH₄⁺. Considering that the
381 Yellow Sea was mainly affected by dust storms from the Hunshandake Desert (Zhang and Gao, 2007),
382 we compared our observations with the sand particles collected from this desert (Table 5). The relative
383 mass concentrations of nitrate and ammonium to the total mass of sand particles were very low, i.e.,
384 less than 81 μg/g, approximately three orders of magnitude less than the corresponding values in our
385 dust samples. Moreover, the values obtained from atmospheric aerosols at Duolun (Cui, 2009) and Alxa
386 Right Banner (Niu and Zhang, 2000) were also more than one order of magnitude lower than the
387 corresponding values in this study (Table 5). This suggested that NO₃⁻ and NH₄⁺ observed in the dust
388 day samples were very likely due to interactions and mixing between anthropogenic air pollutants and
389 dust particles during transport from the source zone to the reception site (Cui et al., 2009; Wang et al.,
390 2011; Wu et al., 2016). However, along the different transport paths of Asian dust, air pollutant
391 emissions, meteorological conditions, chemical reactions, and other factors can affect the abundance of
392 NH₄⁺ and NO₃⁻ in atmospheric particles. These factors can vary greatly among different dust events,
393 hence leading to the three different categories.
394 Considered relative values of NH₄⁺ and NO₃⁻ in dust day sample against in comparison sample, these
395 dust day samples can be classified into three categories. When we focused on inorganic nitrogen (IN),
396 we found that IN concentrations could be grouped into three cases (Table 3). In Category 1, the mass
397 concentrations of NH₄⁺ and NO₃⁻ were larger in dust day sample than in comparison sample. In
398 Category 2, the reverse was true. In Category 3, the mass concentration of NO₃⁻ were less in dust
399 sample higher on dust days than on in comparison sample ND days for Case 1, while IN was lower on
400 dust days for Case 2. For Case 3, nitrate concentration on dust days were less than on ND days, while
401 ammonium concentration on dust days were slightly higher than those on ND days the reverse was true
402 for NH₄⁺.
403 Considering that To understand the influence of dust on the nitrogen concentration, we compared the
404 IN content in aerosols from the coastal region of the Yellow Sea with sand particles and atmospheric
405 aerosols from Duolun, a site very close to the Zhurihe Sand Desert. The Yellow Sea is was mainly
406 affected by dust storms from the Zhurihe Sand desert (this sand source (Zhang and Gao, 2007).), we
407 compared our observation with those sand particles collected at the desert (Table 4). The relative mass
408 concentrations of nitrate and ammonium to the total mass of sand particles were much low, i.e., less

带格式的：行距：1.5 倍行距

带格式的：下标

带格式的：上标

带格式的：下标

带格式的：上标

带格式的：下标

带格式的：上标

409 than 81 μg/g, which were three orders of magnitude less than the corresponding values inherently with
410 our dust samples. Moreover, the values obtained from atmospheric aerosols at Duolun, a site very close
411 to the Zhurihe Sand Desert, in literature (Cui et al., 2009), were also more than one order of magnitude
412 less than the corresponding values in this study (Table 4). This suggested that NO₃⁻ and NH₄⁺ observed
413 in the dust day samples were related to interactions of anthropogenic air pollutants and dust particles
414 during the transport from the source zone to the reception site (Zhang et al., 2016; Cui et al., 2014).
415 However, along the different transport paths of Asian dust, air pollutants' emissions, meteorological
416 conditions, chemical reactions, etc., can affect the abundance of NH₄⁺ and NO₃⁻ in atmospheric
417 particles. These factors could vary a lot in different dust events, leading to three different categories.

418 3.3 Theoretical analysis of three categories

419 Ammonium salts are common in atmospheric particles with diameters of less than 2 μm (Yao et al.,
420 2003; Yao and Zhang, 2012). Gas-aerosol thermodynamic equilibrium is widely assumed to be fully
421 attained for inorganic ions, including ammonium salts in PM_{2.5}, in all regional air quality modeling
422 studies. Reasonably good agreements between ammonium salt modeling results and observations
423 reported in literature support the validity of this assumption (Chen et al., 2016; Penrod et al., 2014;
424 Walker et al., 2012). Assuming that thermodynamic equilibrium had been attained by the ammonium
425 salts in Category 1, the reactions between carbonate salts and ammonium salts, such as 1) (NH₄)₂SO₄+
426 CaCO₃ ⇒ CaSO₄ + NH₃ (gas) + CO₂ (gas) + H₂O and 2) 2NH₄NO₃+ CaCO₃ ⇒ Ca(NO₃)₂ + 2NH₃ (gas)
427 +CO₂ (gas) +H₂O, will release NH₃ (gas) until CaCO₃ has been completely used up. During dust events,
428 much high concentrations of Ca²⁺ were observed, and high CaCO₃ concentrations were therefore
429 expected. When Category 1 was considered alone and one exterior sample was excluded, a good
430 correlation however, was obtained for [NH₄⁺]_{equivalent concentration}=0.98*[NO₃⁻+SO₄²⁻]_{equivalent}
431 concentration (R²=0.83, P<0.05). The good correlation together with the slope of 1 strongly indicated that
432 the NO₃⁻ and SO₄²⁻ were almost completely associated with NH₄⁺ in these dust day samples. The
433 formation of CaSO₄ and/or Ca(NO₃)₂ was probably negligible. Thus, ammonium salt aerosols may
434 externally co-exist with dust aerosols in these dust day samples. In the exterior sample collected on 21
435 March 2010, [NH₄⁺] only accounted for ~70% of the observed [NO₃⁻+SO₄²⁻] in equivalent
436 concentration. This result suggested that ~30% of (NO₃⁻+SO₄²⁻) may be associated with dust aerosols
437 via the formation of metal salts of the two species. The hypothesis was supported by the correlation

438 result, i.e., NO_3^- was positively correlated with NH_4^+ and Cu, and SO_4^{2-} was correlated with K^+ , Na^+ and
439 Mg^{2+} (Fig.S4). Note that only samples in Category 1 showed NH_4^+ to be negatively correlated with
440 Ca^{2+} (Fig.S4).
441 For Category 2, no correlation between $[\text{NH}_4^+]_{\text{equivalent concentration}}$ and $[\text{NO}_3^- + \text{SO}_4^{2-}]_{\text{equivalent concentration}}$
442 existed. When Category 2 was considered alone and one exterior sample was excluded, the equivalent
443 ratios of NH_4^+ to $\text{NO}_3^- + \text{SO}_4^{2-}$ were generally much smaller than 1, suggesting that a larger fraction of
444 $\text{NO}_3^- + \text{SO}_4^{2-}$ may exist as metal salts due to reactions of their precursors with dust aerosols. NO_3^- and
445 SO_4^{2-} showed no correlations with NH_4^+ but did show significant correlations with Pb (Fig.S4),
446 implying that $\text{NO}_3^- + \text{SO}_4^{2-}$ existed as metal salts. The average concentration of Ca^{2+} in Category 2
447 $(0.43 \pm 0.40 \mu\text{g}/\text{m}^3)$ was clearly higher than that in Category 1 (Ca^{2+} : $0.17 \pm 0.04 \mu\text{g}/\text{m}^3$), implying the
448 probable formation of CaSO_4 and/or $\text{Ca}(\text{NO}_3)_2$ and the release of NH_3 (gas), resulting in a decrease in
449 NH_4^+ . However, the concentration of total Ca was $1.11 \pm 0.70 \mu\text{g}/\text{m}^3$ in Category 1 and $0.74 \pm 0.49 \mu\text{g}/\text{m}^3$ in
450 Category 2. In Category 1, NO_3^- was negatively correlated with SO_4^{2-} (Fig.S4), suggesting competition
451 for NH_3 under NH_3 -poor dust days during long-range transport. However, NO_3^- was positively
452 correlated with SO_4^{2-} in Category 2. The latter relationship can be explained by the fact that the amount
453 of CaCO_3 was sufficient to absorb the precursors of both SO_4^{2-} and NO_3^- . Due to the absence of TSP
454 concentration data along the transport pathway, we compared TSP concentrations at the sampling site
455 and found that the average value of Category 2 ($1391 \pm 981 \mu\text{g}/\text{m}^3$) was substantially higher than that of
456 Category 1 ($591 \pm 158 \mu\text{g}/\text{m}^3$). This implied that dust events in Category 2 were even stronger. Note that
457 the NO_2 concentrations in Category 2 ($1.35 \pm 2.45 \mu\text{g}/\text{m}^3$) were lower or comparable to those in
458 Category 1 ($1.51 \pm 2.16 \mu\text{g}/\text{m}^3$). The potential formation of nitrate metal salts was expected to be similar
459 between the two categories, while favorable formation conditions for ammonium nitrate greatly
460 increased the mass concentrations of nitrate and the contributions to the TSPs in Category 1.
461 Overall, the higher ammonium concentrations observed in the dust day samples in Category 1 were
462 likely associated with external co-existence of ammonium salt aerosols. However, the lower
463 concentrations in Category 2 were likely due to unfavorable conditions for forming ammonium salts.
464 The observed ammonium was just the residual of incomplete reactions between preexisting ammonium
465 salt and carbonate salts. More discussion on this issue will be presented in Section 3.4.

466

467 From Table 4, we found that nitrate and ammonium concentrations in the source sand particles were

带格式的：突出显示

468 very low (less than 50 $\mu\text{g/g}$). Therefore, the dust particles in this source area that affect the Yellow
469 Sea are nutrient poor. Although the IN content in aerosols particles at Duolun in dust days was higher
470 than that in sand particles, the nitrate and ammonium concentrations were much lower than those in the
471 coastal region of the Yellow Sea. Other researchers also found the nitrate concentration in dust particles
472 in downwind area higher than that at source region (Zhang et al., 2016; Cui et al., 2014). Therefore, we
473 believe that the dust particles from the source have a dilution effect on atmospheric particulate nitrogen
474 because of the low IN concentration in sand particles, if the dust particles just mixing with
475 anthropogenic particles and no effective heterogeneous reaction on dust particles during the transport.
476 When dust events occurred and no effective formation of nitrate and ammonium reaction happen, the
477 content of nitrogen per particle mass decreased because of the dilution of particulate nitrogen resulting
478 from the increased number of nutrient-poor dust particles rapidly leaving the source area. And we really
479 found some samples in Case 2, such as 20080425, 20080528, 20080529, 20110319 and 20110501, had
480 a lower IN content in aerosols particle on dust days than that on ND. The nitrate concentration decreased
481 30-95% and ammonium decreased 16-72% for these samples. We think these dilution effect resulted by
482 mixing is related with dust intensity of dust events and the distance from the dust source. In the region
483 close to the dust sources, the IN content was very low in aerosols in dust days due to IN-poor dust
484 particles and no effective emission or absorption and reaction occur during such short transport time.
485 However, during long range transport, the concentration of IN will increase by reacting with gas
486 emitted into the air under appropriate reaction conditions or by mixing with anthropogenic aerosol
487 particles from a local source. Therefore, IN concentrations will increase in aerosols in downwind areas
488 because of reactions on the dust surfaces or mixing with anthropogenic particles along the transport
489 path. Cui et al. (2009) observed one dust event at four sites on transport path (Duolun, Beijing, Taishan,
490 Shanghai), and found the enhancement and complex of mixing of dust with anthropogenic particles
491 during transport from source to downwind region. In addition, the dilution effect was affected by dust
492 intensity. For our samples in Case 2, Sample 200805028 corresponded to a severe dust storm; 080529
493 and 110501 was related a dust storm; 110319 was a blowing dust (Table 3). IN concentration decreased
494 by 66-84%, 36-71% and 5-28% for samples collected on severe dust storm, dust storm and blowing dust,
495 respectively. The results showed the stronger a dust storm is and the closer to the source, the
496 stronger the dilution effect is.

497 **Table 34.** Average concentrations of inorganic nitrogen, TSP, NO_x, Relative Humidity (RH) and T for

带格式的: 行距: 1.5 倍行距

498

each case in aerosol samples in the coastal region of the Yellow Sea

499

Sample numbers	TSP $\mu\text{g}\cdot\text{m}^{-3}$	NO_3^- $\mu\text{g}\cdot\text{m}^{-3}$	NH_4^+ $\mu\text{g}\cdot\text{m}^{-3}$	RH %	T $^{\circ}\text{C}$	NO_x $\mu\text{g}\cdot\text{m}^{-3}$	Summary
Case 1	080301, 080315, 090316, 100321, 110415, 110502	696	24.1	14.9	46.6	13.8	62.7 IN>ND
Case 2	080425, 080528, 080529, 110319, 110501	1199	3.1	2.6	29.2	19.8	52.3 IN<ND
Case 3	100315, 100320, 110418	1639	4.9	4.7	10.1	10.1	70.7 NO_3^- <ND NH_4^+ ≅ND
Non-dust		212	5.5	4.6	42.2	13.7	59.7

500

Therefore, IN concentrations will increase in aerosols in downwind areas because of reactions on the

501

dust surfaces or mixing with anthropogenic particles along the transport path. If no effective emission or

带格式的: 段落间距段后: 10 磅, 行距: 1.5 倍行距

带格式的: 段落间距段后: 10 磅, 行距: 1.5 倍行距

带格式的: 段落间距段后: 10 磅, 行距: 1.5 倍行距

带格式的: 两端对齐, 段落间距段后: 10 磅, 行距: 1.5 倍行距, 到齐到网格, 边框: 底端: (无框线), 制表位: 不在 19.78 字符 + 39.55 字符

带格式的: 两端对齐, 段落间距段后: 10 磅, 行距: 1.5 倍行距, 到齐到网格, 边框: 底端: (无框线), 制表位: 不在 19.78 字符 + 39.55 字符

带格式的: 两端对齐, 段落间距段后: 10 磅, 行距: 1.5 倍行距, 到齐到网格, 边框: 底端: (无框线), 制表位: 不在 19.78 字符 + 39.55 字符

带格式的: 段落间距段后: 10 磅, 行距: 1.5 倍行距

502 absorption and reaction occur during transport, the IN content per particle mass ($\mu\text{g/g}$) will decrease in
 503 atmospheric aerosols in the downwind area. In Case 1, the particle concentration in the dust events
 504 was less than $700 \mu\text{g/m}^3$, and the IN concentration in atmospheric aerosols increased by a factor of more
 505 than three in dust events in the coastal region of the Yellow Sea, which might be a result of slow
 506 transport or a weak dilution effect. High relative humidity (RH), low temperature and high
 507 NO_x transport over a long distance and at a low speed are beneficial to the formation of nitrate and
 508 ammonium. In Cases 2 and 3, the particle concentrations were very high, with an average higher than
 509 $1100 \mu\text{g m}^{-3}$, which indicated that the samples were affected by a strong dust storm or that the dust might
 510 be transported quickly. Concentrations of IN in aerosols in dust events decreased at the downwind site
 511 in Case 2 because the low RH, high temperature and low NO_x during rapid transport were not
 512 advantageous to the formation of IN. In Case 3, the low IN content was a result of a strong dilution
 513 effect and low RH.

514 In addition, the transport path affected the IN content of aerosol particles in the downwind area, and
 515 this influence will be discussed in Section 3.3.

516 **Table 45.** Comparison of the IN content in dust particles according to the dust source region (unit: $\mu\text{g/g}$)

Sands sampled in Zhurihe		Aerosols in Duolun*		Aerosols in the coastal region of the Yellow Sea	
NO_3^-	NH_4^+	NO_3^-	NH_4^+	NO_3^-	NH_4^+
25.46±22.87	4.21±1.03	1200	900	Non-dust: 28,200±24,819	Non-dust: 24,063±21,515
				Case 1: 34,892±9570	Case 1: 22,571±7016
				Case 2: 5542±5117	Case 2: 4758±5698

带格式的: 行距: 1.5 倍行距

带格式的: 段落间距段后: 10 磅, 行距: 1.5 倍行距

带格式的: 段落间距段后: 10 磅, 行距: 1.5 倍行距

带格式的: 段落间距段后: 10 磅, 行距: 1.5 倍行距

带格式的: 两端对齐, 段落间距段后: 10 磅, 行距: 1.5 倍行距, 到齐到网格, 边框: 底端: (无框线), 制表位: 不在 19.78 字符 + 39.55 字符

Case 3:

Case 3:

6359+4697

7059+5591

带格式的: 段落间距段后: 10 磅,
行距: 1.5 倍行距

带格式的: 行距: 1.5 倍行距

*Adapted from Cui (2009)

3.3.4 Influence of transport pathways on particulate inorganic nitrogen dust samples

The calculated air mass trajectories of 13 out of 14 samples showed that the air mass originated from Inner Mongolia, China (Fig. 5), generally consistent with the results by Zhang and Gao (2007). The remaining one originated from Northeast China. Figs. 6 and 7 show a few areas with high emissions of NO_x and NH₃, e.g., Liaoning, Beijing-Tianjin-Hebei, Shandong, Henan and Jiangsu in China. The calculated trajectories showed that all the air mass passed over parts of these highly polluted regions and experienced different residence time in these regions. In Fig. 5, except for the one exterior sample, all trajectories in Category 1 showed that the air masses were transported from either the north or northwest over the continent. In Category 2, the air masses crossed over the sea for 94-255 km prior to arriving at the reception site. NH₃-poor conditions in the marine atmosphere disfavored the formation and existence of ammonium nitrate. On the other hand, the humid marine conditions might have enhanced particle-particle coagulation and might have led to the release of NH₃ via reactions between preexisting ammonium salts and carbonate salts. Moreover, we also examined the links among the measured concentrations of particulate ammonium and nitrate, the mixing layer along the back trajectories, and the residence time of air masses crossing over the highly polluted zones. The results supported our hypothesis, i.e., ammonium salts mostly co-existed with dust aerosols externally. For example, except for 20080425, all dust day samples mostly traveled at an altitude above the mixing layer before mixing down to ground level. For most sampling days in Category 1, the average mixing layer was less than 900 m, favoring the trapping of locally emitted anthropogenic air pollutants in the mixing layer. In addition, the air masses at this elevation apparently moved slowly and took over 10 hr to cross over the highly polluted area. Even lower speeds were expected for air masses at the bottom of the mixing layer, as wind speed decreases with height. Except for exterior samples, the sampling days in Category 2 featured a mixing layer that was, on average, higher than 900 m. The air masses at this

542 elevation took less than 10 hr to cross over the highly polluted areas and generally had higher speeds.
543 Theoretically, a lower mixing layer and a lower wind speed favored the accumulation of air pollutants
544 and the formation of ammonium nitrate to some extent. The transport of dust air masses above the
545 mixing layer reduced the possibility for internal mixing of ammonium salts and reaction with dust
546 aerosols along the long transport path. The shorter time for dust air masses mixing down to ground
547 level before arriving at the reception site also increased the possibility for external co-existence
548 between ammonium salt aerosols and dust aerosols in Category 1. The reverse could be argued to
549 explain the observations for Category 2. The correlation analysis results in Table S2 indirectly
550 support these conclusions. In fact, previous studies proposed that nitrate is rarely formed on the surface
551 of dust particles (Zhang and Iwasaka, 1999). Therefore, much lower nitrate concentrations were
552 observed in Category 2. Noted that the exterior samples with ID of 20110415 and 20110502 have not yet been
553 explained.

554
555 ~~The reported threshold of wind speed for dust mobilization in the Gobi Desert ranges from 10–12~~
556 ~~m/s (Choi and Zhang, 2008). We estimated 40.5 ± 9.9 km/h as the average wind speed during a dust storm~~
557 ~~according to Asia dust observations (). If air masses were transported faster than 40.5 km/h, we found~~
558 ~~that the IN content in most atmospheric aerosol samples was lower on dust days than on ND~~
559 ~~days because of the strong dilution effect. This effect was observed in samples 080528, 080529, 110319~~
560 ~~and 100315 (Table 5). If an air mass was transported over the ocean for some distance (ratio of overseas~~
561 ~~to total distance of at least 10%), no matter how fast the transport velocity, the IN content decreased~~
562 ~~because of the input of clean marine air, such as in samples 080425, 100320, 110418 and 110501. If the~~
563 ~~air mass was transported slowly (less than 42.4 km/h) or transported only a short distance over the sea,~~
564 ~~with an overseas to total distance ratio of less than 10%, the IN content increased in samples collected in~~
565 ~~the downwind area, such as in samples 080301, 090316, 100321 and 110502. Therefore, the IN content~~
566 ~~is related to not only the transport path and speed but also local emissions and reaction conditions~~
567 ~~during transport.~~

568 ~~Table 56. IN content, RH, NO_x, transport speed and transport distance over the sea for atmospheric aerosol~~
569 ~~samples on dust days~~

570

Group	Sample-number	TSP ($\mu\text{g}/\text{m}^3$)	NO_3^- ($\mu\text{g}/\text{g}$)	NH_4^+ ($\mu\text{g}/\text{g}$)	Speed (km/h)	Distance-over-the-sea (km)	Ratio-of-the-distance-over-the-sea-to-the-total distance (%)	
Case-1 IN>ND	080304	527	38984	24107	35.1	0	0	
	080315	410	47611	34130	53.4	262	6.8	
	090316	688	23050	25012	59.5	0	0	
	100321	519	31741	18155	49.2	0	0	
	110415	1225	41970	20390	57.0	258	6.3	
Case-2 IN<ND	110502	810	25995	13632	31.2	121	5.4	
	080425	256	4089	372	29.3	253	12.0	
	080528	2579	232	72	79.8	259	4.5	
	080529	2314	26	166	78.0	229	4.1	
	110319	939	13088	10067	55.4	404	10.1	
Case-3	110504	502	8924	10631	30.6	298	13.5	
	100315	501	10767	8515	58.7	183	4.3	
	$\text{NO}_3^- < \text{ND}$	100320	3857	1418	884	38.0	254	9.3
	$\text{NH}_4^+ \cong \text{ND}$	110418	558	6891	11778	23.0	380	22.9

带格式的: 行距: 1.5 倍行距

带格式的: 行距: 1.5 倍行距

带格式的: 行距: 1.5 倍行距

带格式的: 行距: 1.5 倍行距

Figure 6. The 72-h backward trajectories for non-dust (a) and dust (b) samples from 2008 to 2011.

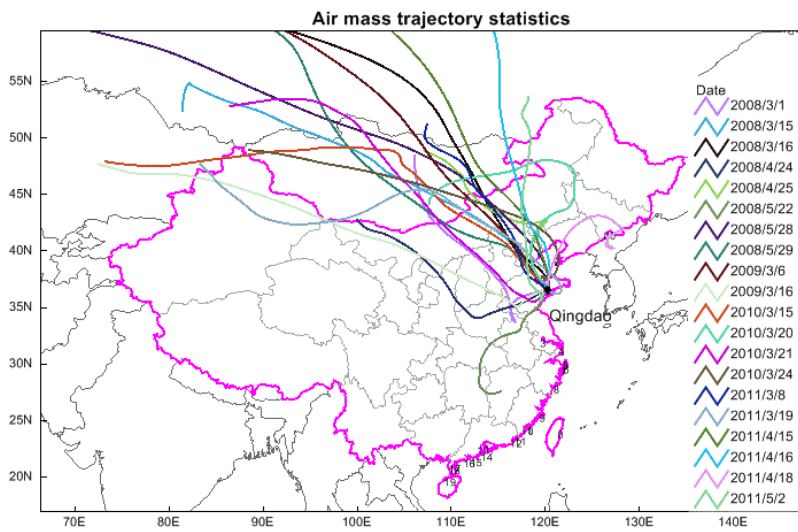
571

572

573

574

575



带格式的: 字体: (默认) Times New Roman, 10 磅

带格式的: 缩进: 首行缩进: 1 字符

带格式的: 行距: 1.5 倍行距

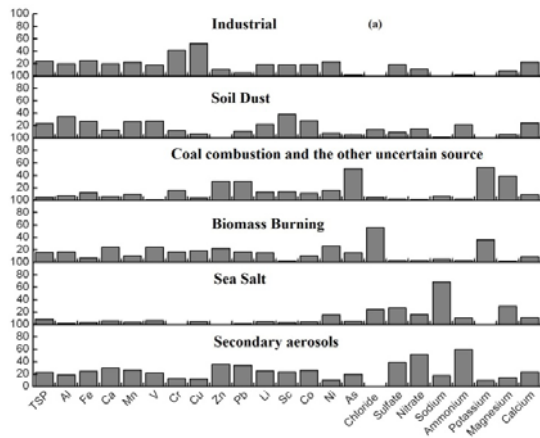
带格式的: 段落间距段后: 10 磅, 行距: 1.5 倍行距

带格式的: 行距: 1.5 倍行距

Figure 4. The 72-h backward trajectories for non-dust and dust samples from 2008 to 2011

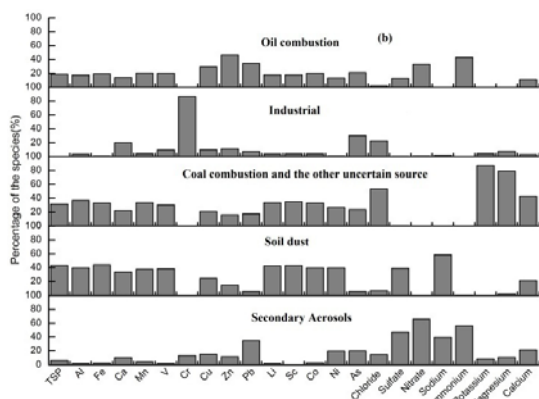
Fig. Daily mean emission of NO_xdust

3.4.5 Source apportionment of aerosols from dust and non-dust events



带格式的: 字体: (默认) Times New Roman, 10 磅

带格式的: 缩进: 首行缩进: 1 字符



带格式的: 字体: (默认) Times New Roman, 10 磅

带格式的: 行距: 1.5 倍行距

Figure 5. Source profiles of atmospheric aerosol samples collected on non-dust (a) and dust (b) days using the PMF model

The sources of atmospheric aerosols on dust and ND days were determined by running the PMF model (Paatero and Tapper, 1993; Paatero, 1997). As shown in Fig. 5, atmospheric aerosols on ND-comparison days were mainly from consisted of six sources: industry, soil dust, secondary aerosols, sea salt, biomass burning, and coal combustion and the other uncertain sources, with 90% of the scaled residuals falling between -3 and +3; $r^2=0.97$. On dust days, the sources of aerosols differed from those on ND days, mainly including oil combustion, industry, soil dust, secondary aerosols, and coal combustion and other uncertain sources. These value are compared in Table 7. We compared the contributions of aerosol sources in dust and ND periods. As shown in Table 6, the contribution of soil dust increased from 23% to 36% on dust days relative to comparison days, which is consistent with the high concentrations of TSPs and crustal metals observed on dust days. Liu et al. (2014) also found an even larger increase in the contribution of dust aerosols to PM_{10} , i.e., 31%-40%, on dust days relative to non-dust days, that the contributions of dust aerosols to PM_{10} increased by 31%-40% on dust days, which is greater than the 10%-20% contribution of local soil dust on ND days. Accordingly, the contributions of local anthropogenic sources decreased on dust day samples, especially those of secondary aerosols, which verified that the influence of anthropogenic sources on atmospheric particulates decreased on dust days. The source profile for coal combustion in dust day samples showed a high percentage of K^+ , Cl, Ca, Mg, Co, Ni, As, Al and Fe, indicating a mixture of coal combustion and other pollutants emitted along the transmission path on dust days. This source increased due to the coal combustion emission mixing with other uncertain source emitted

带格式的: 字体: (默认) Times New Roman, 10 磅

to the air under strong wind. ~~Coal combustion emissions were mainly a mixture of coal combustion and other pollutants emitted along the transmission path on dust days.~~

The calculation results also showed that the contribution of dust aerosol mass (the sum of nitrate and ammonium associated with the dust source) to the total aerosol mass (the total nitrate and ammonium) greatly increased on dust days.

Therefore, the sources of aerosol particles changed on dust days. Dust events had a great impact on aerosol sources in the downwind area. The influence of soil dust on aerosols and IN-loaded particles was greater than that on local sources on dust days. In fact, the contribution of soil dust to aerosols was related to the intensity of the dust storm and the transport path. However, we could not determine the contributions of dust to aerosols for the different dust cases because of the limited number of samples.

Table 6. Sources and source contributions (expressed as %) calculated for aerosol samples collected during dust and non-dust events

Dust event		Non-dust event	
Source	% of TSP	Source	% of TSP
Soil dust	36	Soil dust	23
Industrial	21	Industrial	24
Secondary aerosol	6	Secondary aerosol	23
Oil combustion	6	Biomass burning	16
Coal combustion and other uncertain sources	31	Coal combustion	5
		Sea salt	9

3.5.6 Dry deposition fluxes of aerosol particles TSP, particulate inorganic nitrogen and metals

Dust events are known to increased the concentration and deposition of aerosol particles during long-range transport along the transport path. For example, Fu et al. (2014) found that the long-range transport of dust particles increased the dry deposition of PM₁₀ in the Yangtze River Delta region by a factor of approximately 239820%. Some studies ~~observed~~ reported enhancements in oceanic chlorophyll α following a dust storm events (Tan and Wang, 2014; Banerjee and Kumar, 2014).

带格式的: 行距: 1.5 倍行距

带格式的: 行距: 1.5 倍行距

带格式的: 行距: 1.5 倍行距

带格式的: 行距: 1.5 倍行距

带格式的: 行距: 1.5 倍行距

带格式的: 行距: 1.5 倍行距

带格式的: 行距: 1.5 倍行距

带格式的: 行距: 1.5 倍行距

带格式的: 行距: 1.5 倍行距

带格式的: 字体: 倾斜

623 However, ~~The~~ the deposition ~~magnitude fluxes~~ of dust varied greatly among ~~different~~ dust storms, and
624 only ~~a few some~~ dust episodes were followed by increases in chlorophyll ~~a~~ (Banerjee and Kumar,
625 2014). ~~In addition to those in high-nutrient and low-chlorophyll (HNLC) regions, the input of nitrogen~~
626 ~~input and other nutrients associated with dust deposition is expected to promote the growth of~~
627 ~~phytoplankton. However, the extent can vary greatly depending on the nutrient limitation conditions in~~
628 ~~the oceans. A similar principle holds for the occurrence or absence of algal blooms following dust~~
629 ~~events. Thus, we calculated the dry deposition fluxes of aerosols particles, $N_{NH4+NO3}$ and metal~~
630 ~~elements during dust and comparison periods using the measured component concentrations and~~
631 ~~modeled dry deposition velocities (Table 8). We then compared the dry deposition flux of TSP and~~
632 ~~$N_{NH4+NO3}$ with the previous observations in literature.~~

633 ~~The role of dust deposition as a nutrient source leading to an increase in algal blooms has not been~~
634 ~~adequately addressed. To understand the influence of dust weather on the nitrogen deposition flux, we~~
635 ~~calculated the dry deposition fluxes of aerosols particles, N and metal elements during dust and ND~~
636 ~~periods using the measured component concentrations and modeled dry deposition velocities~~
637 ~~obtained from Williams' model (Qi et al., 2005) (Table 7).~~

638 ~~The dry deposition fluxes of atmospheric particulates increased on dust days relative to comparison~~
639 ~~days. All increases or decreases in this section reflected the value on dust days relative to comparison~~
640 ~~days, if not specified. For example,~~

641 ~~Compared to that on ND days, the dry deposition flux of atmospheric particulate increased on dust~~
642 ~~days. On ND days, the dry deposition flux of ~~particles-TSP~~ was $2,800 \pm 700$ $mg/m^2/month$ in the~~
643 ~~coastal region of the Yellow Sea, and the particle flux varied over a wide range from 5,200-65,000~~
644 ~~$mg/m^2/month$ under different dust ~~conditions~~ sampling days, with an average of ~~+618,800-453~~~~
645 ~~$mg/m^2/month$. The results verified that dust events enhanced the dry deposition flux of atmospheric~~
646 ~~particulates. However, the dry deposition flux of $N_{NH4+NO3}$ did not follow this pattern. It showed~~
647 ~~variations with particles. In Case-Category 1, the dry deposition fluxes of $N_{NH4+NO3}$ increased by a~~
648 ~~factor of 1.19-5.8285%, corresponding to the increase in the TSP flux of 86-252% (Table S3) and the~~
649 ~~flux of atmospheric particles increased by a factor of 1.8-6.3. In Categories 2 and 3, the dry deposition~~
650 ~~fluxes of TSP increased by 126% to 2226% compared to that on comparison days. Except for~~
651 ~~ammonium in Category 3, the dry deposition fluxes of particulate $N_{NH4+NO3}$, however, decreased by 41%~~
652 ~~(on average). A larger relative decrease was found for the concentration of nitrate, i.e., decreases of 73%~~

653 ~~and 46% in Category 2 and 3, respectively. Note that the average ammonium deposition flux decreased~~
654 ~~by 47% in Category 2 but increase in Category 3.~~
655 ~~Cases 2 and 3, the dry deposition flux increased 2.3 to 23.2-fold compared to that on ND days. Except~~
656 ~~for ammonium in Case 3, the dry deposition flux of particulate IN decreased by an average of 41% in~~
657 ~~the case of high particle concentrations. The concentration of nitrate decreased 63% and 46% in Cases~~
658 ~~2 and 3, respectively. Additionally, the ammonium flux decreased by 14% in Case 2, while in Case 3,~~
659 ~~ammonium was higher than that on ND days. We found that dust events sometimes led to an increase~~
660 ~~in the nitrogen input to the ocean relative to that during ND events, but it did not always occur~~
661 ~~depending on the chemical composition of the dust particles. As discussed, dust particles may carry~~
662 ~~abundant reactive nitrogen when they travel through polluted continental atmosphere. However, the~~
663 ~~relatively pure dust particles may be transported when no air pollution occurs along the dust transport~~
664 ~~route to oceans.~~

665 The dry atmospheric deposition fluxes of Fe ~~in atmospheric particulates~~ increased by a factor of
666 ~~2124-2370%~~ on dust days ~~compared to that on ND days.~~ Atmospheric inputs of iron to the ocean ~~can~~
667 ~~have been proposed to~~ enhance primary production in high-nutrient, low-chlorophyll regions (HNLC)
668 areas (Jickells et al., 2005). ~~However~~ Moreover, except for Pb and Zn in Case-Category 2, the dry
669 deposition fluxes of Cu, Pb and Zn increased with those of nitrogen and iron on dust days. ~~These~~ trace
670 metals were found to have a toxic effect on marine phytoplankton and inhibit their growth (Bielmyer et
671 al., 2006; Echeveste et al., 2012). Liu et al. (2013) found that this inhibition coexisted with the
672 promotion of some phytoplankton species in incubation experiments involving the addition of Asian
673 dust samples in the southern Yellow Sea in the spring of 2011. ~~In Case 3, dust was deposited in the ocean,~~
674 ~~the atmospheric supply of nitrogen decreased, and the atmospheric inputs of Fe and some toxic metals~~
675 ~~increased. Moreover, phytoplankton growth was affected by the addition of nutrient elements and toxic~~
676 ~~elements. The overall effect of dust deposition on primary productivity was a combination of these two~~
677 ~~effects. This is likely the reason why inhibition coexisted with the promotion of some phytoplankton~~
678 ~~species in incubation experiments using additions of AD in the southern Yellow Sea in the spring of~~
679 ~~2011 (Liu et al., 2013).~~

680 ~~The contribution of dust events to marine nitrogen input and primary production will be~~
681 ~~overestimated if the nutrient flux simply considers dust concentrations and a constant ratio of nutrients~~
682 ~~to particles. The atmospheric input of nitrogen to the ocean on dust days depends on the 'dilution effect'~~

683 of a dust event. Dust subjected to long-range transport does not always increase the atmospheric input of
 684 nitrogen. Long-term observations of dust events must be performed to evaluate the contributions of dust
 685 to the biogeochemistry of nitrogen and primary production in oceans.

686
 687
 688
 689
 690 **Table 7.** Dry deposition of aerosol particles ($\text{mg}/\text{m}^2/\text{month}$), particulate inorganic nitrogen ($\text{mg N}/\text{m}^2/\text{month}$) and
 691 some toxic trace metals ($\text{mg}/\text{m}^2/\text{month}$) on dust and non-dust days

Dry deposition flux							
	Particles	$\text{NO}_3^- \text{-N}$	$\text{NH}_4^+ \text{-N}$	Fe	Cu	Pb	Zn
Case 1	9600 ± 4300	87 ± 53	25 ± 13	650 ± 340	2 ± 1	0.3 ± 0.2	6 ± 3
IN > ND	4300						
Case 2	$18000 \pm 11,000$	13 ± 18	5 ± 7	1300 ± 1000	3 ± 2	0.08 ± 0.04	4 ± 1
IN < ND	11,000						
Case 3	$29,000 \pm 21,000$	26 ± 6	17 ± 8	2100 ± 2200	6 ± 1	0.20 ± 0.02	5 ± 3
$\text{NO}_3^- < \text{ND}$	31,000						
$\text{NH}_4^+ \approx \text{ND}$							
Non-dust	2800 ± 700	48 ± 33	8 ± 8	190 ± 110	1 ± 1	0.09 ± 0.1	5 ± 4
	700						
This work	2008-2011	Qingdao, coastal region of the Yellow Sea		Non-dust day	2800 ± 700	63 ± 39	
				Dust day	10138 ± 15940	66 ± 61	
Shi et al.,	2007	The Yellow Sea		Non-dust day	192		
	2013						

带格式的: 行距: 1.5 倍行距

带格式的: 行距: 1.5 倍行距

带格式的: 行距: 1.5 倍行距

带格式的: 行距: 1.5 倍行距

带格式的: 行距: 1.5 倍行距

带格式的: 居中, 行距: 1.5 倍行距

带格式的: 行距: 1.5 倍行距

带格式的: 行距: 1.5 倍行距

带格式的: 字体: 小五

带格式的: 居中, 行距: 1.5 倍行距

带格式表格

带格式的: 居中, 行距: 1.5 倍行距

带格式的: 行距: 1.5 倍行距

带格式的: 行距: 1.5 倍行距

带格式的: 居中, 行距: 1.5 倍行距

带格式的: 字体: (中文) + 中文正文, 小五, 非加粗

带格式的: 行距: 1.5 倍行距

带格式的: 字体: 小五

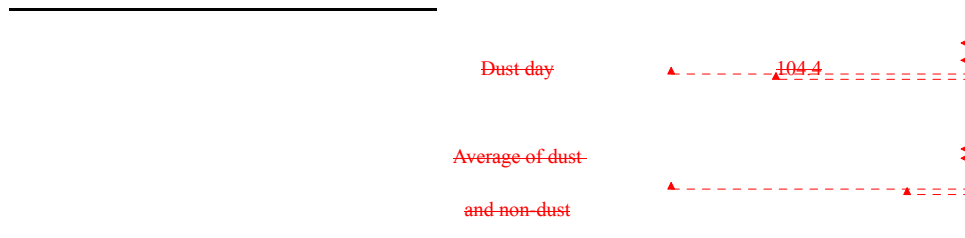
带格式的: 居中, 行距: 1.5 倍行距

带格式的: 行距: 1.5 倍行距

带格式的: 居中, 行距: 1.5 倍行距

带格式的: 字体: 小五

692



- 带格式的: 字体: (中文) +中文正文, 小五, 非加粗
- 带格式的: 行距: 1.5 倍行距
- 带格式的: 居中, 行距: 1.5 倍行距
- 带格式的: 字体: 小五
- 带格式的: 字体: (中文) +中文正文, 小五, 非加粗
- 带格式的: 行距: 1.5 倍行距
- 带格式的: 居中, 行距: 1.5 倍行距
- 带格式的: 字体: 小五
- 带格式的: 字体: 非加粗
- 带格式的: 缩进: 首行缩进: 1 字符, 行距: 1.5 倍行距

693 **3.7 Potential impacts of nitrogen dry deposition flux associated with dust influenced by**
 694 **anthropogenic activity**

695 Due to anthropogenic activity and economic development, inorganic nitrogen emissions increased in
 696 China from 1980 to 2010 (Fig.S5). Accordingly, the $N_{NH4+NO3}$ dry deposition flux should have
 697 theoretically increased with the increase in inorganic nitrogen emissions. However, from the limited
 698 data shown in Table 9, we did not find the expected increase in dry deposition flux of inorganic
 699 nitrogen during the dust days. Considering the uncertainty in dry deposition velocity, we normalized
 700 the dry deposition flux of $N_{NH4+NO3}$ using the concentration of nitrate and ammonium reported in the
 701 literature and the recommended dry deposition velocity of 1 cm/s for nitrate and 0.1 m/s for ammonium
 702 in coastal areas reported by Duce et al. (1991). We then found that dry deposition fluxes of $N_{NH4+NO3}$
 703 over the Yellow Sea during the dust days increased greatly from 1999 to 2007. The fluxes of
 704 $N_{NH4+NO3}$ in Qingdao, including during the dust days, varied narrowly in a range of 94.75-99.65 mg
 705 $N/m^2/month$ from 1997 to 2011(Table 8). The complicated results may reflect the combined effects of
 706 NO_x and NH_3 emissions in northern China, the occurrence frequency and intensity of dust events and
 707 metrological conditions affecting the transport pathways and moving speeds of dust air masses and
 708 chemical reactions occurring therein. For example, dust events commonly exhibited a periodic
 709 variation from 2000 to 2011 (Fig.S5).

710 **4 Conclusion**

711 The concentrations of nitrate and ammonium in TSP samples varied greatly from event to event on
 712 dust days. Relative to non-dust day samples, the concentrations were both higher in some cases and
 713 lower in others. The observed ammonium in dust day samples was explained by ammonium salt
 714 aerosols co-existing externally with dust aerosols or the residual of incomplete reactions between
 715 ammonium salts and carbonate salts. NO_3^- in the dust day samples was partially related to mixing and
 716 reactions between anthropogenic air pollutants and dust particles during the transport from the source
 717 zone to the reception site. However, this process was generally much less effective and led to a sharp
 718 decrease in nitrate in Category 2 TSP samples. The external co-existence of ammonium salt aerosols

带格式的: 行距: 1.5 倍行距

719 with dust aerosols and the extent of the reactions between ammonium salts and carbonate salts were
720 apparently associated with the transport pathway, moving speeds and metrological conditions, among
721 other factors.

722

723 The concentration of ~~particulate IN~~ nitrate and ammonium in TSP samples varied greatly~~exhibited a~~
724 large variation from event to event on dust days, ~~and a dust event did not simply increase nutrient~~
725 concentrations. Relative to non-dust day samples, the concentrations were both higher in some cases
726 and lower in others. The observed ammonium in dust day samples was explained by ammonium salt
727 aerosols co-existing externally with dust aerosols or the residual of incomplete reactions between
728 ammonium salts and carbonate salts. NO₃⁻ in the dust day samples was partially related to mixing and
729 reactions between anthropogenic air pollutants and dust particles during the transport from the source
730 zone to the reception site. However, this process was generally much less effective and led to a sharp
731 decrease in nitrate in Category 2 TSP samples. The external co-existence of ammonium salt aerosols
732 with dust aerosols and the extent of the reactions between ammonium salts and carbonate salts were
733 apparently associated with the transport pathway, moving speeds and metrological conditions, among
734 other factors.

735 ~~The effect of dust events on particulate nitrogen in the downwind region was determined by the~~
736 ~~dilution effect of a dust event, which depends on many factors, such as the dust storm intensity,~~
737 ~~transport speed and path, local source emissions during transport, meteorological state and atmospheric~~
738 ~~reactions. Due to a sharp increase in dust loads on dust days, the contribution of soil dust to the total~~
739 aerosol mass was higher on dust days than on comparison days, while the contributions from local
740 anthropogenic sources were accordingly lower.

741

742 ~~Dust events affect the source apportionment of aerosols. The contribution of soil dust to aerosols~~
743 ~~increased, while local anthropogenic sources decreased during a dust event. The contribution of dust to~~
744 ~~aerosols must be studied further under different IN conditions.~~

745 Overall, this study strongly suggested that atmospheric deposition of N_{NH4++NO3-} on dust days varied
746 greatly and that no simple linear increase existed with increasing dust load. More observations at
747 various locations are needed to obtain a statistical relationship between dust events and atmospheric
748 deposition of N_{NH4++NO3-}. A simple assumption of a linear increase in N_{NH4++NO3-} with increasing dust
749 load, like that in the literature, could lead to considerable overestimation of the dry deposition flux of

带格式的: 行距: 1.5 倍行距

带格式的: 字体: (默认) Times
New Roman

750 ~~nutrients into the oceans and the consequent primary production associated with dust events.~~
751 ~~Dust events enhance the input of atmospheric particulates via dry deposition. However, the influence~~
752 ~~of dust events on the input of nitrogen to the ocean is still uncertain. The dry deposition flux of IN on~~
753 ~~dust days decreased when a strong dilution effect was present. The contribution of dust events to~~
754 ~~marine nitrogen inputs and primary production could be overestimated if the dry deposition flux of~~
755 ~~nutrients is estimated using only particulate concentrations on dust days.~~

756

757 *Acknowledgments.* This work was supported by the Department of Science and Technology of the P. R. China
758 through the State Key Basic Research & Development Program under Grant No. 2014CB953701 and the National
759 Natural Science Foundation of China (No. 41375143). ~~We thank Prof. Yaqiang Wang and Jinhui Shi for the~~
760 ~~valuable discussion regarding this research. We also express our appreciation to Tianran Zhang for help with sand~~
761 ~~sampling and Qiang Zhang for data collection. We thank Prof. Xiaohong Yao for the valuable discussion regarding~~
762 ~~this research. We also express our appreciation to Tianran Zhang for help with sand sampling.~~

763 **References**

764 Banerjee, P., and Prasanna Kumar, S.: Dust-induced episodic phytoplankton blooms in the Arabian Sea
765 during winter monsoon, *Journal of Geophysical Research Oceans*, 119, 7123–7138, 2014.
766 Bielmyer, G. K., Grosell, M., and Brix, K. V.: Toxicity of silver, zinc, copper, and nickel to the copepod
767 *Acartia tonsa* exposed via a phytoplankton diet, *Environmental science & technology*, 40, 2063–2068,
768 2006.
769 Choi H., Zhang Y. H.: Predicting dust storm evolution with the vorticity theory, *Atmospheric Research*,
770 89, 338–350, 2008.
771 Cui W. L.: Chemical transformation of dust components and mixing mechanisms of dust with pollution
772 aerosols during the long range transport from north to south China, M.S. thesis, Department of
773 Environmental Science and Engineering, Fudan University, 32–38 pp., 2009.
774 Duce, R. A., and Zamora, L.: Impacts of atmospheric anthropogenic nitrogen on the open ocean,
775 *Science*, 320, 893–897, 2008.
776 Echeveste, P., Agustí, S., and Tovar-Sánchez, A.: Toxic thresholds of cadmium and lead to oceanic
777 phytoplankton: cell size and ocean basin dependent effects, *Environmental Toxicology and*

带格式的: 行距: 1.5 倍行距

778 Chemistry, 31, 1887–1894, 2012.

779 EPA, U.: Method 1631, Revision E: Mercury in water by oxidation, purge and trap, and cold vapor
780 atomic fluorescence spectrometry, US Environmental Protection Agency Washington, DC, 2002.

781 Fitzgerald, E., Ault, A. P., Zauseher, M. D., Mayol-Bracero, O. L., and Prather, K. A.: Comparison of
782 the mixing state of long-range transported Asian and African mineral dust, *Atmospheric
783 Environment*, 115, 19–25, 2015.

784 Fu, X., Wang, S. X., Cheng, Z., Xing, J., Zhao, B., Wang, J. D., and Hao, J. M.: Source, transport and
785 impacts of a heavy dust event in the Yangtze River Delta, China, in 2011, *Atmospheric Chemistry &
786 Physics*, 14, 1239–1254, 2014.

787 Guo, C., Yu, J., Ho, T. Y., Wang, L., Song, S., Kong, L., and Liu, H.: Dynamics of phytoplankton
788 community structure in the South China Sea in response to the East Asian aerosol input,
789 *Biogeosciences*, 9, 1519–1536, 2012.

790 Han, X.: Air Quality Modeling for of a Strong Dust Event in East Asia in March 2010, *Aerosol & Air
791 Quality Research*, 12, 615–628, 2012.

792 He Q., Wei W., Li X., Aili M., Li S.: Profile Characteristics of Wind Velocity, Temperature
793 and Humidity in the Surface Layer during a Sandstorm Passing Taklimakan Desert Hinterland, *Desert
794 and Oasis Meteorology*, 2(6), 6–11, 2008.

795 Hsu, S. C., Liu, S. C., Huang, Y. T., Lung, S. C. C., Tsai, F., Tu, J. Y., and Kao, S. J.: A criterion for
796 identifying Asian dust events based on AI concentration data collected from northern Taiwan
797 between 2002 and early 2007, *Journal of Geophysical Research Atmospheres*, 113, 1044–1044, 2008.

798 Jaafar, M., Baalbaki, R., Mrad, R., Daher, N., Shihadeh, A., Sioutas, C., and Saliba, N. A.: Dust
799 episodes in Beirut and their effect on the chemical composition of coarse and fine particulate matter,
800 *Science of the Total Environment*, 496C, 75–83, 2014.

801 Jekells, T., An, Z., Andersen, K. K., Baker, A., Bergametti, G., Brooks, N., Cao, J., Boyd, P., Duce, R.,
802 and Hunter, K.: Global iron connections between desert dust, ocean biogeochemistry, and climate,
803 *science*, 308, 67–71, 2005.

804 KaiZhang, ZK., and Gao, H.: The characteristics of Asian dust storms during 2000–2002: From the
805 source to the sea, *Atmospheric Environment*, 41, 9136–9145, 2007.

806 Kang, E., Han, J., Lee, M., Lee, G., and Kim, J. C.: Chemical characteristics of size-resolved aerosols
807 from Asian dust and haze episode in Seoul Metropolitan City, *Atmospheric Research*, 127, 34–46,

808 2013.

809 Li N., Liu Z., Yang H., Wu J., Lei Y.: Change of wind speed and soil moisture during occurrence of
810 dust storms, *Journal of Natural Disasters*, 15(6), 28-32, 2006.

811 Li, W., Shao, L., Shi, Z., Chen, J., Yang, L., Yuan, Q., Yan, C., Zhang, X., Wang, Y., and Sun, J.:
812 Mixing state and hygroscopicity of dust and haze particles before leaving Asian continent, *Journal of*
813 *Geophysical Research Atmospheres*, 119, 1044-1059, 2014.

814 Lin, X., Liu, C., and Zhang, H.: Determination of Metal Elements in Aerosol by ICP-AES, *Rock &*
815 *Mineral Analysis*, 1998, 17(2): 143-146.

816 Liu, Q., and Bei, Y.: Impacts of crystal metal on secondary aliphatic amine aerosol formation during
817 dust storm episodes in Beijing, *Atmospheric Environment*, 128, 227-334, 2016.

818 Liu, Q., Liu, Y., Yin, J., Zhang, M., and Zhang, T.: Chemical characteristics and source apportionment
819 of PM 10 during Asian dust storm and non-dust storm days in Beijing, *Atmospheric Environment*, 91,
820 85-94, 2014.

821 Liu, Y., Zhang, T. R., Shi, J. H., Gao, H. W., and Yao, X. H.: Responses of chlorophyll a to added
822 nutrients, Asian dust, and rainwater in an oligotrophic zone of the Yellow Sea: Implications for
823 promotion and inhibition effects in an incubation experiment, *Journal of Geophysical Research*
824 *Biogeosciences*, 118, 1763-1772, 2013.

825 Ma, Q., Liu, Y., Liu, C., Ma, J., and He, H.: A case study of Asian dust storm particles: Chemical
826 composition, reactivity to SO₂ and hygroscopic properties, *Journal of Environmental Sciences*, 24,
827 62-71, 2012.

828 Natsagdorj L., Jugder D., Chung Y. S.: Analysis of dust storms observed in Mongolia during 1937-1999,
829 *Atmospheric Environment*, 37, 1401-1411, 2003.

830 Paatero, P., and Tapper, U.: Analysis of different modes of factor analysis as least-squares-fit problems,
831 *Chemometrics and Intelligent Laboratory Systems*, 18, 183-194, 1993.

832 Paatero, P.: Least-squares formulation of robust non-negative factor analysis,
833 *Chemometrics & Intelligent Laboratory Systems*, 37, 23-35, 1997.

834 Qi, J. H., Gao, H. W., Yu, L. M., and Qiao, J. J.: Distribution of inorganic nitrogen-containing species
835 in atmospheric particles from an island in the Yellow Sea, *Atmospheric Research*, 101, 938-955,
836 2011.

837 Qi, J. H., Shi, J. H., Gao, H. W., and Sun, Z.: Atmospheric dry and wet deposition of nitrogen species

838 and its implication for primary productivity in coastal region of the Yellow Sea, China, *Atmospheric*
839 *Environment*, 81, 600-608, 2013.

840 Qi, J., Li, P., Li, X., Feng, L., and Zhang, M.: Estimation of dry deposition fluxes of particulate species
841 to the water surface in the Qingdao area, using a model and surrogate surfaces, *Atmospheric*
842 *Environment*, 39, 2081-2088, 2005.

843 Shi, J. H., Gao, H. W., Zhang, J., Tan, S. C., Ren, J. L., Liu, C. G., Liu, Y., and Yao, X.: Examination of
844 causative link between a spring bloom and dry/wet deposition of Asian dust in the Yellow Sea, China,
845 *Journal of Geophysical Research Atmospheres*, 117, 127-135, 2012.

846 Tan, S. C., and Wang, H.: The transport and deposition of dust and its impact on phytoplankton growth
847 in the Yellow Sea, *Atmospheric Environment*, 99, 491-499, 2014.

848 Wang, L., Du, H., Chen, J., Zhang, M., Huang, X., Tan, H., Kong, L., and Geng, F.: Consecutive
849 transport of anthropogenic air masses and dust storm plume: Two case events at Shanghai, China,
850 *Atmospheric Research*, 127, 22-33, 2013.

851 Wang, Q., Zhuang, G., Huang, K., Liu, T., Lin, Y., Deng, C., Fu, Q., Fu, J. S., Chen, J., and Zhang, W.:
852 Evolution of particulate sulfate and nitrate along the Asian dust pathway: Secondary transformation
853 and primary pollutants via long range transport, *Atmospheric Research*, 169, 86-95, 2015.

854 Wang, Y. Q., Zhang, X. Y., and Draxler, R. R.: TrajStat: GIS-based software that uses various trajectory
855 statistical analysis methods to identify potential sources from long term air pollution measurement
856 data, *Environmental Modelling & Software*, 24, 938-939, 2009.

857 XIN, W. c., LIN, X. h., and XU, L.: ICP-MS Determination of 34 Trace Elements in Marine Sediments
858 [J], *Physical Testing and Chemical Analysis (Part B: Chemical Analysis)*, 4, 029, 2012.

859 Xu, J., Wang, Z., Yu, G., Qin, X., Ren, J., and Qin, D.: Characteristics of water-soluble ionic species in
860 fine particles from a high-altitude site on the northern boundary of Tibetan Plateau: Mixture of
861 mineral dust and anthropogenic aerosol, *Atmospheric Research*, 143, 43-56, 2014.

862 Yang, D., Yan, P., and Xu, X.: Characteristics of aerosols under dust and sand weather in Beijing,
863 *Quarterly Journal of Applied Meteorology/Meteorology*, 2002S1, 185-194, 2002.

864 Zhan, K., Zhao, M., Fang, E., Yang, Z., Zhang, Y., Guo, S., Zhang, J., Wang, Q., and Wang, D.: The
865 wind speed characteristics of near surface vertical gradient of 50m in sandstorm process in 2006,
866 *Journal of Arid Land Resources & Environment*, 23, 100-105, 2009.

867 Zhang, W., Zhuang, G., Huang, K., Li, J., Zhang, R., Wang, Q., Sun, Y., Fu, J. S., Chen, Y., and Xu, D.:

868 [Mixing and transformation of Asian dust with pollution in the two dust storms over the northern](#)
869 [China in 2006, Atmospheric Environment, 44, 3394-3403, 2010.](#)

870 [Zhang, Y., Yu, Q., Ma, W., and Chen, L.: Atmospheric deposition of inorganic nitrogen to the eastern](#)
871 [China seas and its implications to marine biogeochemistry, Journal of Geophysical Research](#)
872 [Atmospheres, 115, 3421-3423, 2010.](#)

873 [Banerjee, P., and Kumar, P. S.: Dust-induced episodic phytoplankton blooms in the Arabian Sea](#)
874 [during winter monsoon, J. Geophys. Res-Oceans., 119, 7123-7138, 2014.](#)

875 [Bielmyer, G. K., Grosell, M., and Brix, K. V.: Toxicity of silver, zinc, copper, and nickel to the](#)
876 [copepod *Acartiatonsa* exposed via a phytoplankton diet, Environ. Sci. Technol., 40, 2063-2068,](#)
877 [2006.](#)

878 [Chen, D., Liu, Z. Q., Fast, J., and Ban, J. M.: Simulations of sulfate–nitrate–ammonium \(SNA\)](#)
879 [aerosols during the extreme haze events over northern china in october 2014, Atmos. Chem.](#)
880 [Phys., 16, 10707-10724, 2016.](#)

881 [CMA: Regulations of Surface Meteorological Observation, China Meteorological Press, Beijing,](#)
882 [154–156, 2004.](#)

883 [CMA: Sand-dust weather almanac 2011, China Meteorological Press, Beijing, 36-53, 2013.](#)

884 [Cui, W. L., Guo, R., and Zhang, H.: The Long-range Transport of Dust from Mongolia/Gobi to the](#)
885 [Yangtze River Basin and its Mixing with Pollutant Aerosols, Journal of Fudan University](#)
886 [\(Natural Science\), 48, 585-592, 2009a.](#)

887 [Cui, W. L.: Chemical transformation of dust components and mixing mechanisms of dust with](#)
888 [pollution aerosols during the long range transport from north to south China, M.S. thesis,](#)
889 [Department of Environmental Science and Engineering, Fudan University, China, 38 pp.,](#)
890 [2009b.](#)

891 [Dai, Y.J.: Vertical distribution of characteristics of dust aerosols in the near-surface in hinterland of](#)
892 [Taklimakan Desert, M.S. thesis, College of Resources and Environmental Science, Xinjiang](#)
893 [University, China, 26 pp., 2016.](#)

894 [Duce, R. A., LaRoche, J., Altieri, K., Arrigo, K. R., Baker, A. R., Capone, D. G., Cornell,](#)
895 [S., Dentener, F., Galloway, J., Ganeshram, R. S., Geider, R. J., Jickells, T., Kuypers, M.](#)
896 [M., Langlois, R., Liss, P. S., Liu, S. M., Middelburg, J. J., Moore, C. M., Nickovic, S., Oschlies, A.,](#)
897 [Pedersen, T., Prospero, J., Schlitzer, R., Seitzinger, S., Sorensen, L. L., Uematsu, M., Ulloa, O.,](#)
898 [Voss, M., Ward, B., and Zamora, L.: Impacts of atmospheric anthropogenic nitrogen on the](#)
899 [open ocean, Science, 320, 893-897, 2008.](#)

900 [Duce, R. A., Liss, P. S., Merrill, J. T., Atlas, E. L., Buat-Menard, P., Hicks, B. B., Miller, J. M.,](#)
901 [Prospero, J. M., Arimoto, R., Church, T. M., Ellis, W., Galloway, J. N., Hansen, L., Jickells, T.](#)
902 [D., Knap, A. H., Reinhardt, K. H., Schneider, B., Soudine, A., Tokos, J. J., Tsunogai, S., Wollast](#)
903 [R., and Zhou, M. Y.: The atmospheric input of trace species to the world ocean, Global](#)
904 [Biogeochem. Cy., 5, 193-259, 1991.](#)

905 [Echeveste, P., Agustí, S., and Tovar-Sánchez, A.: Toxic thresholds of cadmium and lead to oceanic](#)
906 [phytoplankton: cell size and ocean basin-dependent effects, Environ. Toxicol. Chem., 31,](#)
907 [1887–1894, 2012.](#)

908 [Fitzgerald, E., Ault, A. P., Zauscher, M. D., Mayol-Bracero, O. L., and Prather, K. A.: Comparison](#)
909 [of the mixing state of long-range transported Asian and African mineral dust, Atmos. Environ.,](#)

910 [115, 19-25, 2015.](#)

911 [Fu, X., Wang, S. X., Cheng, Z., Xing, J., Zhao, B., Wang, J. D., and Hao, J. M.: Source, transport](#)

912 [and impacts of a heavy dust event in the Yangtze River Delta, China, in 2011, Atmos. Chem.](#)

913 [Phys., 14, 1239-1254, 2014.](#)

914 [Grice, S., Stedman, J., Kent, A., Hobson, M., Norris, J., Abbott, J., and Cooke, S.:Recent trends](#)

915 [and projections of primary NO₂emissions in Europe, Atmos. Environ., 43, 2154-2167, 2009.](#)

916 [Guo, C., Yu, J., Ho, T. Y., Wang, L., Song, S., Kong, L., and Liu, H.: Dynamics of phytoplankton](#)

917 [community structure in the South China Sea in response to the East Asian aerosol input,](#)

918 [Biogeosciences, 9, 1519-1536, 2012.](#)

919 [Han, X., Ge, C., Tao, J. H., Zhang, M. G., and Zhang, R. J.: Air Quality Modeling for of a Strong](#)

920 [Dust Event in East Asia in March 2010, Aerosol. Air. Qual. Res., 12, 615-628, 2012.](#)

921 [Jickells, T. D., An, Z. S., Andersen, K. K., Baker, A. R., Bergametti, G., Brooks, N., Cao, J. J.,](#)

922 [Boyd, P. W., Duce, R. A., Hunter, K., Kawahata, H., Kubilay, N., laRoche, J., Liss, P. S.,](#)

923 [Mahowald, N., Prospero, J. M., Ridgwell, A. J., Tegen, I., and Torres, R.: Global iron](#)

924 [connections between desert dust, ocean biogeochemistry, and climate, Science, 308, 67-71,](#)

925 [2005.](#)

926 [Kang, E., Han, J., Lee, M., Lee, G., and Kim, J. C.: Chemical characteristics of size-resolved](#)

927 [aerosols from Asian dust and haze episode in Seoul Metropolitan City, Atmos. Res., 127, 34-46,](#)

928 [2013.](#)

929 [Li, W. J., Shao, L. Y., Shi, Z. B., Chen, J. M., Yang, L. X., Yuan, Q., Yan, C., Zhang, X. Y., Wang,](#)

930 [Y. Q., Sun, J. Y., Zhang, Y. M., Shen, X. J., Wang, Z. F., and Wang, W. X.: Mixing state and](#)

931 [hygroscopicity of dust and haze particles before leaving Asian continent, J. Geophys.](#)

932 [Res-Atmos, 119, 1044–1059, 2014.](#)

933 [Lin, X. H., Liu, C. L., and Zhang, H.: Determination of Metal Elements in Aerosol by ICP-AES,](#)

934 [Rock & Mineral Analysis, 17, 143-146, 1998.](#)

935 [Liu, L., Zhang, X. Y., Xu W., Liu, X. J., Li, Y., Lu, X. H., Zhang, Y. H., and Zhang, W. T.:](#)

936 [Temporal characteristics of atmospheric ammonia and nitrogen dioxide over China based on](#)

937 [emission data, satellite observations and atmospheric transport modeling since 1980, Atmos.](#)

938 [Chem. Phys., 106, 1-32, 2017.](#)

939 [Liu, Q. Y., and Bei, Y. L.: Impacts of crystal metal on secondary aliphatic amine aerosol formation](#)

940 [during dust storm episodes in Beijing, Atmos. Environ., 128, 227-334, 2016.](#)

941 [Liu, Q. Y., Liu, Y. J., Yin, J. X., Zhang, M. G., and Zhang, T. T.: Chemical characteristics and](#)

942 [source apportionment of PM 10 during Asian dust storm and non-dust storm days in Beijing,](#)

943 [Atmos. Environ., 91, 85-94, 2014.](#)

944 [Liu, X. H., Zhang, Y., Cheng, S. H., Xing, J., Zhang, Q., Streets, D. G., Jang, C., Wang, W. X., and](#)

945 [Hao, J. M.: Understanding of regional air pollution over China using CMAQ, part I](#)

946 [performance evaluation and seasonal variation, Atmos. Environ., 44, 2415-2426, 2010a.](#)

947 [Liu, X. H., Zhang, Y., Xing, J., Zhang, Q., Wang, K., Streets, D. G., Jang, C., Wang, W. X., and Hao,](#)

948 [J. M.: Understanding of regional air pollution over China using CMAQ, part II. Process analysis](#)

949 [and sensitivity of ozone and particulate matter to precursor emissions, Atmos. Environ., 44,](#)

950 [3719-3727, 2010b.](#)

951 [Liu, Y., Zhang, T. R., Shi, J. H., Gao, H. W., and Yao, X. H.: Responses of chlorophyll a to added](#)

952 [nutrients, Asian dust, and rainwater in an oligotrophic zone of the Yellow Sea: Implications for](#)

953 [promotion and inhibition effects in an incubation experiment, J. Geophys. Res-Bioge., 118,](#)

954 [1763-1772, 2013.](#)

955 [Ma, Q. X., Liu, Y. C., Liu, C., Ma, J. Z., and He, H.: A case study of Asian dust storm particles:](#)

956 [Chemical composition, reactivity to SO₂ and hygroscopic properties, J. Environ. Sci., 24, 62-71,](#)

957 [2012.](#)

958 [Mori, I., Nishikawa, M., Tanimura, T., and Quan, H.: Change in size distribution and chemical](#)

959 [composition of kosa \(Asian dust\) aerosol during long-range transport, Atmos. Environ., 37,](#)

960 [4253-4263, 2003.](#)

961 [Niu, S. J., and Zhang, C. C.: Researches on Sand Aerosol Chemical Composition and Enrichment](#)

962 [Factor in the Spring at Helan Mountain Area, Journal of Desert Research, 20, 264-268, 2000.](#)

963 [Ohara, T., Akimoto, H., Kurokawa, J., Horii, N., Yamaji, K., Yan, X., and Hayasaka, T.: An Asian](#)

964 [emission inventory of anthropogenic emission sources for the period 1980–2020, Atmos.](#)

965 [Chem. Phys., 7, 4419-4444, 2007.](#)

966 [Paatero, P., and Tapper, U.: Analysis of different modes of factor analysis as least squares fit](#)

967 [problems, Chemometr. Intell. Lab., 18, 183-194, 1993.](#)

968 [Paatero, P.: Least squares formulation of robust non-negative factor analysis, Chemometr. Intell.](#)

969 [Lab., 37, 23-35, 1997.](#)

970 [Penrod, A., Zhang, Y., Wang, K., Wu, S. Y. and Leung, L. R.: Impacts of future climate and](#)

971 [emission changes on U.S. air quality, Atmos. Environ., 89, 533-547, 2014.](#)

972 [Qi, J. H., Gao, H. W., Yu, L. M., and Qiao, J. J.: Distribution of inorganic nitrogen-containing](#)

973 [species in atmospheric particles from an island in the Yellow Sea, Atmos. Res., 101, 938-955,](#)

974 [2011.](#)

975 [Qi, J. H., Li, P. L., Li, X. G., Feng, L. J., and Zhang, M. P.: Estimation of dry deposition fluxes of](#)

976 [particulate species to the water surface in the Qingdao area, using a model and surrogate](#)

977 [surfaces, Atmos. Environ., 39, 2081-2088, 2005.](#)

978 [Qi, J. H., Shi, J. H., Gao, H. W., and Sun, Z.: Atmospheric dry and wet deposition of nitrogen](#)

979 [species and its implication for primary productivity in coastal region of the Yellow Sea, China,](#)

980 [Atmos. Environ., 81, 600-608, 2013.](#)

981 [Sheng, Y., Yang, S., Han, Y., Zheng, Q., and Fang, X.: The concentrations and sources of nitrate in](#)

982 [aerosol over Dolmud, Qinghai, China, Journal of Desert Research, 36, 792-797, 2016.](#)

983 [Shi, J. H., Gao, H. W., Zhang, J., Tan, S. C., Ren, J. L., Liu, C. G., Liu, Y., and Yao, X. H.:](#)

984 [Examination of causative link between a spring bloom and dry/wet deposition of Asian dust in](#)

985 [the Yellow Sea, China, J. Geophys. Res-Atmos., 117, 127-135, 2012.](#)

986 [Shi, J. H., Zhang, J., Gao, H. W., Tan, S. C., Yao, X. H., and Ren, J. L.: Concentration, solubility](#)

987 [and deposition flux of atmospheric particulate nutrients over the Yellow Sea, Deep-sea. Res. Pt.](#)

988 [II, 97, 43–50, 2013.](#)

989 [Skjøth C. A., and Hertel, O.: Ammonia Emissions in Europe, Urban Air Quality in Europe,](#)

990 [Springer Berlin Heidelberg, The Handbook of Environmental Chemistry, Germany, 163 pp.,](#)

991 [2013.](#)

992 [Tan, S. C., and Wang, H.: The transport and deposition of dust and its impact on phytoplankton](#)

993 [growth in the Yellow Sea, Atmos. Environ., 99, 491-499, 2014.](#)

994 [Taylor, S. R.: Abundance of chemical elements in the continental crust: a new table, Geochim.](#)

995 [Cosmochim. Ac., 28, 1273-1285, 1964.](#)

996 [U. S., EPA.: Method 1631, Revision E: Mercury in water by oxidation, purge and trap, and cold](#)

997 [vapor atomic fluorescence spectrometry, US Environmental Protection Agency Washington, DC,](#)

998 [2002.](#)

999 [Uno, I., Carmichael, G. R., Streets, D. G., Tang, Y., Yienger, J. J., Satake, S., Wang, Z., Woo, J. H.,](#)

1000 [Guttikunda, S., Uematsu, M., Matsumoto, K., Tanimoto, H., Yoshioka, K., and Iida, T.:](#)

1001 [Regional chemical weather forecasting system CFORS: Model descriptions and analysis of](#)

1002 [surface observations at Japanese island stations during the ACE-Asia experiment, *J. Geophys.*](#)

1003 [Res-Atmos., 108, 1147-1164, 2003.](#)

1004 [Walker, J. M., Philip, S., Martin, R. V., and Seinfeld, J. H.: Simulation of nitrate, sulfate, and](#)

1005 [ammonium aerosols over the United States, *Atmos. Chem. Phys.*, 12, 11213-11227, 2012.](#)

1006 [Wang, L., Du, H. H., Chen, J. M., Zhang, M., Huang, X. Y., Tan, H. B., Kong, L. D., and Geng, F.](#)

1007 [H.: Consecutive transport of anthropogenic air masses and dust storm plume: Two case events](#)

1008 [at Shanghai, China, *Atmos. Res.*, 127, 22-33, 2013.](#)

1009 [Wang, Q. Z., Zhuang, G. S., Huang, K., Liu, T. N., Lin, Y. F., Deng, C. R., Fu, Q. Y., Fu, J. S.,](#)

1010 [Chen, J. K., Zhang, W. J., and Yiming, M.: Evolution of particulate sulfate and nitrate along the](#)

1011 [Asian dust pathway: Secondary transformation and primary pollutants via long-range transport,](#)

1012 [Atmos. Res., 169, 86-95, 2016.](#)

1013 [Wang, Q. Z., Zhuang, G. S., Li, J., Huang, K., Zhang, R., Jiang, Y. L., Lin, Y. F., and Fu, J. S.:](#)

1014 [Mixing of dust with pollution on the transport path of Asian dust — Revealed from the aerosol](#)

1015 [over Yulin, the north edge of Loess Plateau, *Sci. Total. Environ.*, 409, 573–581, 2011.](#)

1016 [Wang, Y. Q., Zhang, X. Y., and Draxler, R. R.: TrajStat: GIS-based software that uses various](#)

1017 [trajectory statistical analysis methods to identify potential sources from long-term air pollution](#)

1018 [measurement data, *Environ. Modell. Softw.*, 24, 938-939, 2009.](#)

1019 [Wang, Y. Q., Zhang, X. Y., Gong, S. L., Zhou, C. H., Hu, X. Q., Liu, H. L., Niu, T., and Yang, Y.](#)

1020 [Q.: Surface observation of sand and dust storm in East Asia and its application in CUACE/Dust,](#)

1021 [Atmos. Chem. Phys., 8, 545–553, 2008.](#)

1022 [Wang, Z., Pan, X. L., Uno, I., Li, J., Wang, Z. F., Chen, X. S., Fu, P. Q., Yang, T., Kobayashi, H.,](#)

1023 [Shimizu, A., Sugimoto, N., and Yamamoto, S.: Significant impacts of heterogeneous reactions](#)

1024 [on the chemical composition and mixing state of dust particles: A case study during dust events](#)

1025 [over northern China, *Atmos. Environ.*, 159, 83-91, 2017.](#)

1026 [Williams, R. W.: A model for the dry deposition of particles to natural water surface. *Atmos.*](#)

1027 [Environ., 16, 1933-1938, 1982.](#)

1028 [Wu, F., Zhang, D. Z., Cao, J. J., Guo, X., Xia, Y., Zhang, T., Lu, H., and Cheng, Y.: Limited](#)

1029 [production of sulfate and nitrate on front-associated dust storm particles moving from desert to](#)

1030 [distant populated areas in northwestern China, *Atmos. Chem. Phys.*, 8, 1-22, 2016.](#)

1031 [Xin, W. C., Lin, X. H., and Xu, L.: ICP-MS Determination of 34 Trace Elements in Marine](#)

1032 [Sediments, *Physical Testing and Chemical Analysis \(Part B: Chemical Analysis\)*, 4, 29, 2012.](#)

1033 [Xu, J. Z., Wang, Z. B., Yu, G. M., Qin, X., Ren, J. W., and Qin, D. H.: Characteristics of water](#)

1034 [soluble ionic species in fine particles from a high altitude site on the northern boundary of](#)

1035 [Tibetan Plateau: Mixture of mineral dust and anthropogenic aerosol, *Atmos. Res.*, 143, 43-56,](#)

1036 [2014.](#)

1037 [Yang, D. Z., Wang, C., Wen, Y. P., Yu, X. L., and Xiu, X. B.: An analysis of Two Sand Storms In](#)

1038 [Spring 1990, *Quarterly Journal of Applied Meteorology*, 6, 18-26, 1995.](#)

1039 [Yang, D. Z., Yan, P., and Xu, X. D.: Characteristics of aerosols under dust and sand weather in](#)

1040 [Beijing, *Quarterly Journal of Applied Meteorology*, 1, 185-194, 2002.](#)

1041 [Yao, X. H., and Zhang, L.: Supermicron modes of ammonium ions related to fog in rural](#)

1042 [atmosphere. Atmos. Chem. Phys., 12, 11165-11178, 2012.](#)

1043 [Yao, X. H., Lau, A. S., Fang, M., Chan, C., and Hu, M.: Size Distributions and Formation of Ionic](#)

1044 [Species in Atmospheric Particulate Pollutants in Beijing, China: 1—Inorganic Ions. Atmos.](#)

1045 [Environ., 37, 2991-3000, 2003.](#)

1046 [Zhang, D., and Iwasaka, Y.: Nitrate and sulfate in individual Asian dust-storm particles in Beijing,](#)

1047 [China in spring of 1995 and 1996, Atmos. Environ., 33, 3213-3223, 1999.](#)

1048 [Zhang, G. S., Zhang, J., and Liu, S. M.: Characterization of nutrients in the atmospheric wet and](#)

1049 [dry deposition observed at the two monitoring sites over Yellow Sea and East China Sea, J.](#)

1050 [Atmos. Chem., 57, 42-57, 2007.](#)

1051 [Zhang, J., Zhang, G. S., Bi, Y. F., and Liu, S. M.: Nitrogen species in rainwater and aerosols of the](#)

1052 [Yellow and East China seas: Effects of the East Asian monsoon and anthropogenic emissions](#)

1053 [and relevance for the NW Pacific Ocean, Global Biogeochem. Cy., 25, 113-120, 2011.](#)

1054 [Zhang, K., and Gao, H. W.: The characteristics of Asian-dust storms during 2000–2002: From the](#)

1055 [source to the sea, Atmos. Environ., 41, 9136-9145, 2007.](#)

1056 [Zhang, Q., Streets, D. G., Carmichael, G. R., He, K. B., Huo, H., Kannari, A., Klimont, Z., Park, I.](#)

1057 [S., Reddy, S., Fu, J. S., Chen, D., Duan, L., Lei, Y., Wang, L. T., and Yao, Z. L.: Asian emissions](#)

1058 [in 2006 for the NASA INTEX-B mission. Atmos. Chem. Phys., 9, 5131-5153, 2009.](#)

1059 [Zhang, W. J., Zhuang, G. S., Huang, K., Li, J., Zhang, R., Wang, Q. Z., Sun, Y. L., Fu, J. S., Chen,](#)

1060 [Y., and Xu, D. Q.: Mixing and transformation of Asian dust with pollution in the two dust](#)

1061 [storms over the northern China in 2006, Atmos. Environ., 44, 3394-3403, 2010a.](#)

1062 [Zhang, Y., Yu, Q., Ma, W. C., and Chen, L. M.: Atmospheric deposition of inorganic nitrogen to](#)

1063 [the eastern China seas and its implications to marine biogeochemistry, J. Geophys. Res-Atmos,](#)

1064 [115, 3421-3423, 2010b.](#)

带格式的: 行距: 1.5 倍行距

1067
1068
1069
1070
1071
1072
1073
1074
1075
1076
1077
1078
1079

1080
1081
1082
1083
1084
1085
1086
1087
1088
1089

Table 1. Sampling information for the aerosol samples collected at the Baguanshan site in the coastal region of the Yellow Sea.

<u>Sampling Year</u>	<u>Sample category</u>	<u>Sampling number</u>	<u>Sampling time</u>	<u>Weather characteristics</u>	
<u>2008</u>	<u>Samples on dust days</u>	<u>20080301</u>	<u>From 13:22 a.m. to 17:22 p.m. on Mar. 1st</u>	<u>Floating dust^a</u>	
		<u>20080315</u>	<u>From 13:21 a.m. to 17:21 p.m. on Mar. 15th</u>	<u>Floating dust</u>	
		<u>20080425</u>	<u>From 13:14 a.m. to 17:14 p.m. on Apr. 25th</u>	<u>Floating dust</u>	
		<u>20080528</u>	<u>From 11:38 a.m. to 15:38 p.m. on May 28th</u>	<u>Floating dust</u>	
		<u>20080529</u>	<u>From 10:15 a.m. to 12:15 p.m. on May 29th^b</u>	<u>Floating dust</u>	
	<u>Samples on non-dust days</u>	<u>20080316</u>	<u>From 13:00 a.m. to 17:00 p.m. on Mar. 16th</u>	<u>Sunny day</u>	
		<u>20080424</u>	<u>From 13:00 a.m. to 17:00 p.m. on Apr. 24th</u>	<u>Sunny day</u>	
		<u>20080522</u>	<u>From 13:00 a.m. to 17:00 p.m. on May 22nd</u>	<u>Cloudy day with mist</u>	
	<u>2009</u>	<u>Samples on dust days</u>	<u>20090316</u>	<u>From 8:25 a.m. to 12:25 p.m. on Mar. 16th</u>	<u>Floating dust</u>
		<u>Samples on non-dust days</u>	<u>20090306</u>	<u>From 13:00 a.m. to 17:00 p.m. on Mar. 6th</u>	<u>Sunny day</u>
<u>2010</u>	<u>Samples on dust days</u>	<u>20100315</u>	<u>From 11:30 a.m. to 15:30 p.m. on Mar. 16th</u>	<u>Mist after floating dust</u>	
		<u>20100320</u>	<u>From 10:30 a.m. to 14:30 p.m. on Mar. 20th</u>	<u>Floating dust</u>	
		<u>20100321</u>	<u>From 10:30 a.m. to 14:30 p.m. on Mar. 21st</u>	<u>Floating dust</u>	
	<u>Samples on non-dust days</u>	<u>20100324</u>	<u>From 11:30 a.m. to 15:30 p.m. on Mar. 24th</u>	<u>Sunny day</u>	

	<u>non-dust days</u>	<u>p.m. on Mar. 24th</u>		
<u>2011</u>	<u>20110319</u>	<u>From 12:00 a.m. to 16:00 p.m. on Mar. 19th</u>	<u>Floating dust</u>	
	<u>20110415</u>	<u>From 12:00 a.m. to 16:00 p.m. on Apr. 15th</u>	<u>Floating dust</u>	
	<u>Samples on dust days</u>	<u>20110418</u>	<u>From 12:25 a.m. to 16:25 p.m. on Apr. 18th</u>	<u>Floating dust^c</u>
		<u>20110501</u>	<u>From 12:10 a.m. to 16:10 p.m. on May 1st</u>	<u>Floating dust</u>
		<u>20110502</u>	<u>From 16:00 a.m. to 20:00 p.m. on May 2nd</u>	<u>Floating dust</u>
		<u>20110308</u>	<u>From 12:00 a.m. to 16:00 p.m. on Mar. 8th</u>	<u>Sunny day</u>
	<u>Samples on non-dust days</u>	<u>20110416</u>	<u>From 12:00 a.m. to 16:00 p.m. on Apr. 16th</u>	<u>Sunny day</u>
		<u>20110523</u>	<u>From 12:00 a.m. to 16:00 p.m. on May 23rd</u>	<u>Sunny day</u>

1090 ^aNote that one exterior dust sample was collected on March 1 when no dust was recorded by the
1091 MICAPS. However, the MICAPS information indeed showed dust events in China on March 1. The
1092 modeled spatial distribution of the PM₁₀ mass concentration for this dust event on March 1 implies that
1093 the sample should be classified as a dust sample. The supporting figure is Fig. S1.

1094 ^bThe sampling duration was reduced to only 2 hrs because of extremely high particle loads.

1095 ^cNote that one exterior dust sample was collected on April 18 when no dust was recorded by the
1096 MICAPS. However, blowing dust occurred and was recorded on April 17 by the Sand-dust weather
1097 almanac 2011 (CMA, 2013). The modeled spatial distribution of the PM₁₀ mass concentration for this
1098 dust event on April 18 implies that the sample should be classified as a dust sample. The supporting
1099 figure is Fig. S2.

1100
1101
1102
1103
1104
1105
1106
1107
1108
1109
1110
1111
1112
1113
1114
1115
1116

1117
1118
1119
1120
1121
1122
1123
1124
1125
1126
1127
1128
1129

1130

Table 2. Detection limits, precisions and recoveries of water-soluble ions and metal elements.

<u>Component</u>	<u>Measurement method</u>	<u>Detection limit ($\mu\text{g}\cdot\text{L}^{-1}$)</u>	<u>Precision (RSD%)</u>	<u>Recovery (%)</u>
<u>NO₃⁻</u>	<u>IC</u>	<u>2.72</u>	<u>1.54</u>	<u>97</u>
<u>SO₄²⁻</u>		<u>1.62</u>	<u>1.55</u>	<u>98</u>
<u>NH₄⁺</u>		<u>0.4</u>	<u>1.10</u>	<u>97</u>
<u>Ca²⁺</u>		<u>0.44</u>	<u>0.79</u>	<u>94</u>
<u>Cu</u>	<u>ICP-MS (Xin et al., 2012)</u>	<u>0.006</u>	<u>4.0</u>	<u>106</u>
<u>Zn</u>		<u>0.009</u>	<u>2.5</u>	<u>102</u>
<u>Cr</u>		<u>0.004</u>	<u>3.0</u>	<u>95</u>
<u>Sc</u>		<u>0.002</u>	<u>2.4</u>	<u>97</u>
<u>Pb</u>		<u>0.008</u>	<u>3.9</u>	<u>104</u>
<u>Al</u>	<u>ICP-AES (Lin et al., 1998)</u>	<u>7.9</u>	<u>0.6</u>	<u>103</u>
<u>Ca</u>		<u>5.0</u>	<u>1.2</u>	<u>99</u>
<u>Fe</u>		<u>2.6</u>	<u>0.7</u>	<u>104</u>
<u>Na</u>		<u>3.0</u>	<u>0.6</u>	<u>99</u>
<u>Mg</u>		<u>0.6</u>	<u>0.6</u>	<u>105</u>
<u>Hg</u>		<u>CVAFS</u>	<u>0.0001</u>	<u>6.6</u>
<u>As</u>	<u>0.1</u>		<u>5.0</u>	<u>98</u>

1131
1132
1133
1134
1135
1136
1137
1138
1139
1140
1141

1142
 1143
 1144
 1145
 1146
 1147
 1148
 1149
 1150
 1151
 1152
 1153
 1154
 1155
 1156
 1157
 1158
 1159
 1160
 1161
 1162
 1163
 1164
 1165
 1166
 1167
 1168
 1169
 1170
 1171
 1172

Table 3. The average concentrations and EFs of metal elements on dust and non-dust days.

Element	Concentration (ng/m ³)		EF*	
	Non-dust days	Dust days	Non-dust days	Dust days
Sc	1.11	13.90	-	-
Al	8.53×10 ³	6.86×10 ⁴	3.8	1.4
Fe	4.91×10 ³	3.88×10 ⁴	3.	1.2
Ca	1.05×10 ⁴	4.29×10 ⁴	14.0	2.1
Mg	1.62×10 ³	1.58×10 ⁴	3.5	1.1
Cu	50.2	124.5	36.3	6.1
Pb	127.9	221.0	389.4	56.1
Zn	340.0	457.7	248.9	20.6
Cr	33.8	244.0	44.0	11.1
Hg	0.26	0.36	176.0	13.8
As	25.5	27.4	707.2	43.9

*EF values less than 10 indicate that the studied element is derived mainly from crustal sources, whereas EF values much higher than 10 indicate an anthropogenic source.

1173
1174
1175
1176
1177
1178
1179
1180
1181
1182
1183
1184
1185
1186
1187
1188

Table 4. Average concentrations of inorganic nitrogen (DIN), TSP, NO_x, relative humidity (RH) and air temperature for each aerosol sample category in Qingdao.

Sample number	TSP μg·m ⁻³	NO ₃ ⁻ μg·m ⁻³	NH ₄ ⁺ μg·m ⁻³	RH %	T °C	NO _x μg·m ⁻³	Summary
20080301	527	20.5	12.7	57	7.0	36	
20080315	410	19.5	29.9	62	11.0	59	<u>DIN concentration on dust days higher than that on non-dust days</u>
Category 1 20090316	688	15.9	17.2	27	16.0	75	
20100321	519	16.5	9.4	51	8.8	76	
20110502	810	21.0	11.0	49	17.7	62	
20080425	622	6.8	2.0	30	18.0	40	<u>DIN concentration on dust days lower than that on non-dust days</u>
20080528	2579	9.2	2.7	17	27.0	34	
Category 2 20080529	2314	17.5	4.8	60	20.0	29	
20110319	939	12.3	9.4	16	12.6	93	
20110501	502	4.5	5.3	23	21.6	66	
20100315	501	5.4	4.3	30	7.2	73	<u>NO₃⁻ concentration on dust days lower than that on non-dust days; NH₄⁺ close to that on non-dust days</u>
Category 3 20100320	3857	5.5	3.4	35	10.6	92	
20110418	558	3.8	6.6	33	12.6	47	
20080316	225	12.6	8.4	28	11.0	60	<u>Non-dust^a</u>
20080424	137	21.7	7.2	49	18.0	53	
20080522	206	27.4	16.6	78	20.0	60	

20090306	94	2.9	3.0	29	7.00	51
20100324	275	7.2	2.4	23	9.0	82
20110308	194	13.0	13.1	20	11.5	111
20110416	252	5.6	5.4	26	14.1	55
20110523	224	15.2	10.2	42	20.6	49

^aFor the corresponding non-dustday for each dust event, see Table 1.

Table 5. Comparison of the inorganic nitrogen (DIN) content in sand and aerosol particles on dust days or close to the dust source region (unit: $\mu\text{g/g}$)

Sands sampled in dust source regions	Aerosols in or close to dust source region on dust days						Aerosols in the coastal region of the Yellow Sea	
	Relative concentration ^a		Study region and data source	Relative concentration ^a		NO ₃ ⁻	NH ₄ [±]	
	NO ₃ ⁻	NH ₄ [±]		NO ₃ ⁻	NH ₄ [±]			
Zhurihe (This study)	25.46±22.87	4.21±1.03	Duolun (Cui, 2009)	1200	900	Non-dust: 28,200±24,819	Non-dust: 24,063±21,515	
AlxaLeftBanner, Inner Mongolia (NiuandZhang, 2000)	62.1±7.4	79.1±1.1	AlxaRightBanner, Inner Mongolia (NiuandZhang, 2000)	1975^b	4091^b	Category 1: 34,892±9570	Category 1: 22,571±7,016	
Yanchi, Ningxia (NiuandZhang, 2000)	46.4±2.2	80.9±1.3	Hinterland of theTaklimakan Desert, Xinjiang (Dai et al., 2016)	142-233	2-15	Category 2: 5,542±5,117	Category 2: 4,758±5,698	
			Average of SonidYouqi, Huade (Inner Mongolia), Zhangbei (Hebei) (Mori et al., 2003)	253	710	Category 3: 6,359±4,697	Category 3: 7,059±5,591	

<u>Yulin, the north edge</u>		
<u>of Loess Plateau</u>	<u>216.4</u>	<u>80.6</u>
<u>(Wang et al., 2011)</u>		
<u>Golmud,</u>		
<u>Qinghai(Sheng et al.,</u>	<u>892.9</u>	<u>±^c</u>
<u>2016)</u>		
<u>Hohhot, Inner</u>		
<u>Mongolia (Yang et al.,</u>	<u>588.1</u>	<u>No data</u>
<u>1995)</u>		

1197 ^aRelative concentration of DIN per aerosol particle mass
1198 ^b Samples collected on a floating dust day (Horizontal visibility less than 10000 m and very low wind speed)
1199 ^c The ammonium concentration was lower than the detection limit of the analytical instrument

1200
1201
1202
1203
1204
1205
1206
1207
1208

Table 6. Concentrations of TSP, NO₃⁻, and NH₄⁺; transport speed; transport distance over the sea; transport distance; air temperature; RH; average mixed layer during transport and transport time in polluted region for atmospheric aerosol samples on dust days.

Group	Sample number	TSP (μg/m ³)	NO ₃ ⁻ (μg/g)	NH ₄ ⁺ (μg/g)	Speed (km/h)	Distance over the sea (km)	Transport altitude (m)	Mixed layer depth (m)	Residence time ^a (h)	T ^b (°C)	RH (%)	
Category 1	080301	527	38.984	24.107	40.1	0	1,160±702	864±745	39	-2.9±11.7	29±10	
	080315	410	47.611	34.130	79.1	0	4,921±1,870	950±525	13	-32.5±16.4	34±16	
	IN>ND	090316	688	23.050	25.012	86.2	0	3,739±1083	702±665	11	-19.1±11.7	42±17
	100321	519	31.741	18.155	87.2	0	3,407±1,249	1,113±760	19	-23.0±13.6	42±22	
	110502	810	25.995	13.632	30.2	177	3,666±1,371	747±957	26	-13.2±15.8	31±13	
Category 2	080425	256	4.089	372	29.6	0	887±656	1,161±1,040	10	-2.7±6.1	66±13	
	080528	2579	232	72	88.2	244	4,336±1,461	1,064±830	8	-15.5±13.6	31±16	
	IN<ND	080529	2314	26	166	63.7	94	2,148±1,725	1,194±816	43	3.6±18.4	25±17
	110319	939	13,088	10,067	70.6	132	4,271±1,867	790±719	27	-26.3±20.0	48±32	
	110501	502	8.924	10.631	35.1	252	3,212±810	916±1,114	5	-13.4±8.5	39±13	

Category 3	<u>100315</u>	<u>501</u>	<u>10.767</u>	<u>8.515</u>	<u>57.3</u>	<u>0</u>	<u>5.009±1410</u>	<u>1.110±365</u>	<u>7</u>	<u>-40.4±13.3</u>	<u>45±29</u>
<u>NO₃⁻<ND</u>	<u>100320</u>	<u>3857</u>	<u>1.418</u>	<u>884</u>	<u>76.9</u>	<u>0</u>	<u>1.284±401</u>	<u>525±371</u>	<u>10</u>	<u>-12.2±6.3</u>	<u>61±16</u>
<u>NH₄⁺≡ND</u>	<u>110418</u>	<u>558</u>	<u>6.891</u>	<u>11.778</u>	<u>35.6</u>	<u>931</u>	<u>1.344±780</u>	<u>695±672</u>	<u>2</u>	<u>-0.1±8.2</u>	<u>52±28</u>

1209
1210
1211
1212
1213
1214
1215
1216
1217
1218
1219
1220
1221
1222
1223
1224
1225

Table 7. Sources and source contributions (expressed in%) calculated for aerosol samples collected during dust and non-dust events

<u>Dust event</u>		<u>Comparison days</u>	
<u>Source</u>	<u>% of TSP</u>	<u>Source</u>	<u>% of TSP</u>
<u>Soil dust</u>	<u>36</u>	<u>Soil dust</u>	<u>23</u>
<u>Industrial</u>	<u>21</u>	<u>Industrial</u>	<u>24</u>
<u>Secondary aerosol</u>	<u>6</u>	<u>Secondary aerosol</u>	<u>23</u>
<u>Oil combustion</u>	<u>6</u>	<u>Biomass burning</u>	<u>16</u>
<u>Coal combustion and other uncertain sources</u>	<u>31</u>	<u>Coal combustion</u>	<u>5</u>
		<u>Sea salt</u>	<u>9</u>

1226
1227
1228
1229
1230
1231
1232
1233
1234
1235
1236
1237
1238

1239
 1240
 1241
 1242
 1243
 1244
 1245
 1246
 1247
 1248
 1249
 1250
 1251
 1252
 1253
 1254
 1255
 1256
 1257
 1258
 1259
 1260
 1261
 1262
 1263
 1264
 1265
 1266
 1267
 1268
 1269
 1270

Table 8. Dry deposition of TSP (mg/m²/month), particulate inorganic nitrogen (mg N/m²/month) and some toxic trace metals (mg/m²/month) on dust and non-dust days.

	Dry deposition flux							
	TSP	NO ₃ ⁻ -N	NH ₄ ⁺ -N	N _{NH4++NO3-}	Fe	Cu	Pb	Zn
Category 1 ^a	8,000± 1800	65±9	24±14	90±17	533±179	2±0.3	0.3±0.3	6±2
Category 2 ^a	18000± 11,000	13±18	8±4	21±22	1300±100 0	3±2	0.08±0.04	4±1
Category 3 ^a	29,000± 31,000	26±6	17±8	42±12	2100±220 0	6±1	0.20±0.02	5±3
Non-dust	2,800± 700	48±33	15±8	63±39	190±110	1±1	0.09±0.1	5±4

^aFor the characterization of N_{NH4++NO3-} concentration and sample information of the category, see in Table 3.

1271
1272
1273
1274
1275
1276
1277
1278
1279
1280
1281
1282
1283
1284
1285
1286
1287
1288
1289
1290
1291

Table 9. Comparison of dry deposition flux and normalized flux of TSP (mg/m²/month) and N_{NH4++NO3-} (mg N/m²/month) with observations from other studies(mg N/m²/month)

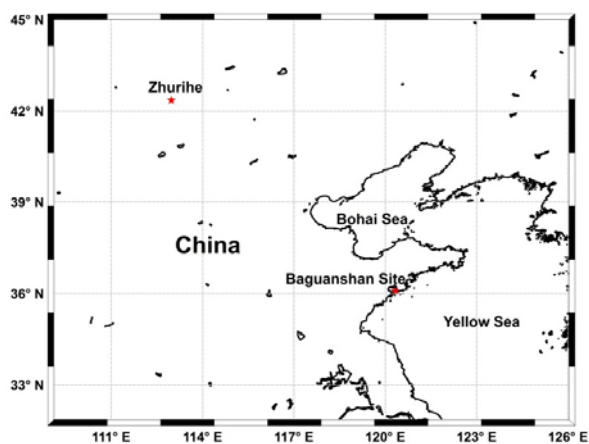
<u>Source</u>	<u>Year</u>	<u>Area</u>	<u>TSP</u>	<u>N_{NH4++NO3-}</u>	<u>Normalized average flux of N_{NH4++NO3-}^a</u>	
<u>This work</u>	<u>2008-2011</u>	<u>Qingdao, coastal region of the Yellow Sea</u>	<u>Non-dust day</u>	<u>2,800±700</u>	<u>63±39</u>	<u>93.90</u>
			<u>Dust day</u>	<u>10,138±15,940</u>	<u>58±36</u>	<u>101.39</u>
			<u>Average of dust and non-dust</u>			<u>97.64</u>
<u>Qi et al., 2013</u>	<u>2005-2006</u>	<u>Qingdao, coastal region of the Yellow Sea</u>	<u>Average of nine months samples</u>	<u>159.2 - 3,172.9</u>	<u>1.8-24.5</u>	<u>94.75</u>
<u>Zhang et al., 2011</u>	<u>1997-2005</u>	<u>Qingdao</u>	<u>Average of annual samples</u>		<u>132</u>	<u>99.65</u>
<u>Zhang et al., 2007</u>	<u>1999-2003</u>	<u>The Yellow Sea</u>			<u>11.43</u>	<u>9.91</u>
<u>Shi et al., 2013</u>	<u>2007</u>	<u>The Yellow Sea</u>	<u>Non-dust day</u>		<u>19.2</u>	<u>132.17</u>
			<u>Dust day</u>		<u>104.4</u>	<u>227.07</u>

Average of dust
and non-dust

179.62

1292
1293
1294
1295
1296
1297
1298
1299

^a The calculation method of normalized flux of $N_{\text{NH}_4^{++}\text{NO}_3^-}$ was discussed in section 3.7.



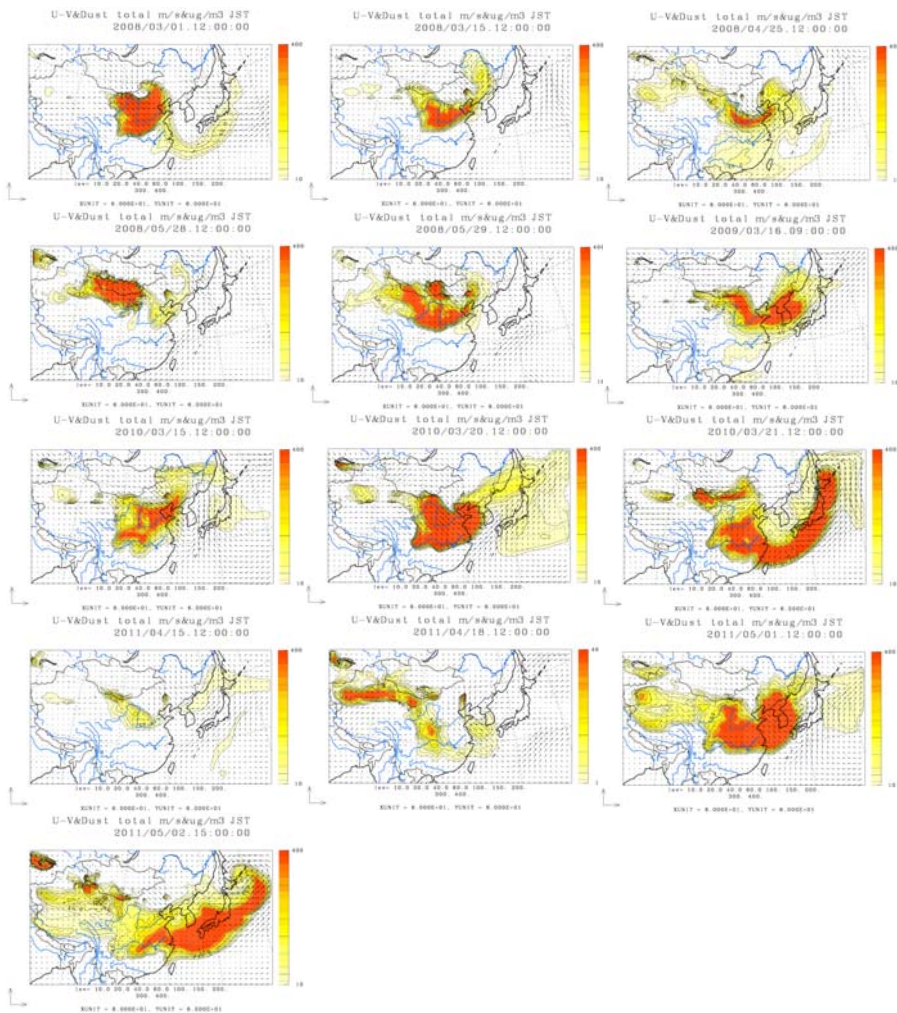
带格式的: 字体: (默认) Times
New Roman

1300
1301

Figure 1. Location of the aerosol and dust sampling sites.

1302
1303
1304
1305
1306
1307
1308
1309
1310
1311
1312
1313
1314
1315
1316
1317
1318
1319
1320

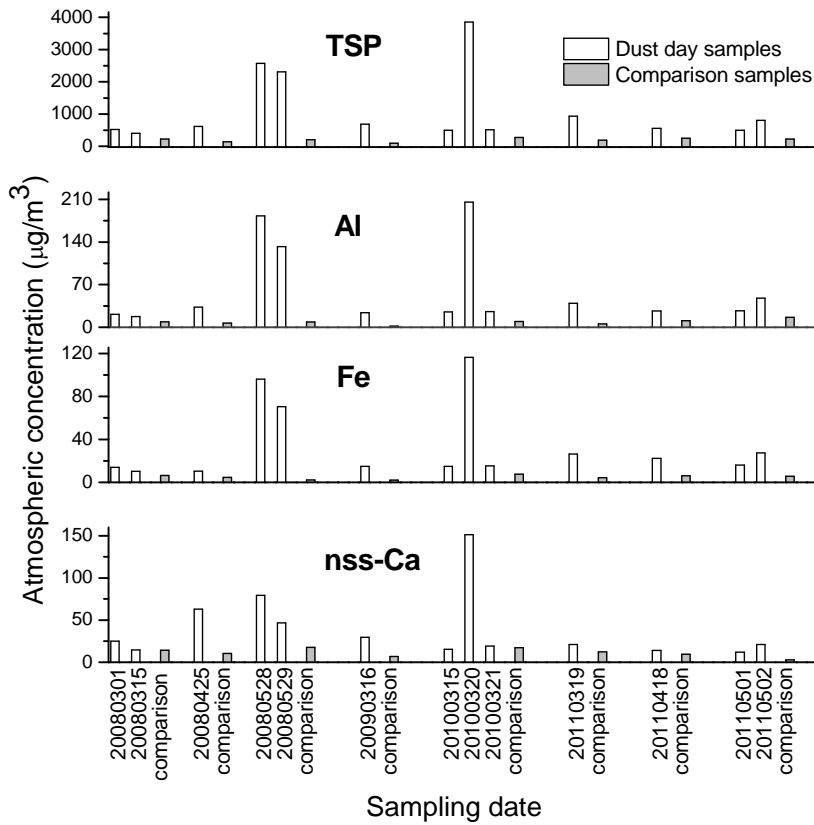
1321
 1322
 1323
 1324
 1325
 1326
 1327
 1328
 1329
 1330
 1331
 1332
 1333



1334 **Figure 2.** Modeled dust concentrations over East Asia by CFORS model during each dust sampling day
 1335 from 2008 to 2011 (<http://www-cfors.nies.go.jp/>). (The figures show the modeled dust concentration
 1336 in the middle of each sampling duration). Nodata are available for Mar. 19, 2011, because of the

1337 [earthquake in Japan.Hourly PM10 concentrationsweremodeled by the WRF-CMAQ model for](#)
 1338 [eachsampling day.and the resultsareshownin Fig. S3.](#)

1339
 1340
 1341
 1342
 1343
 1344
 1345
 1346
 1347
 1348

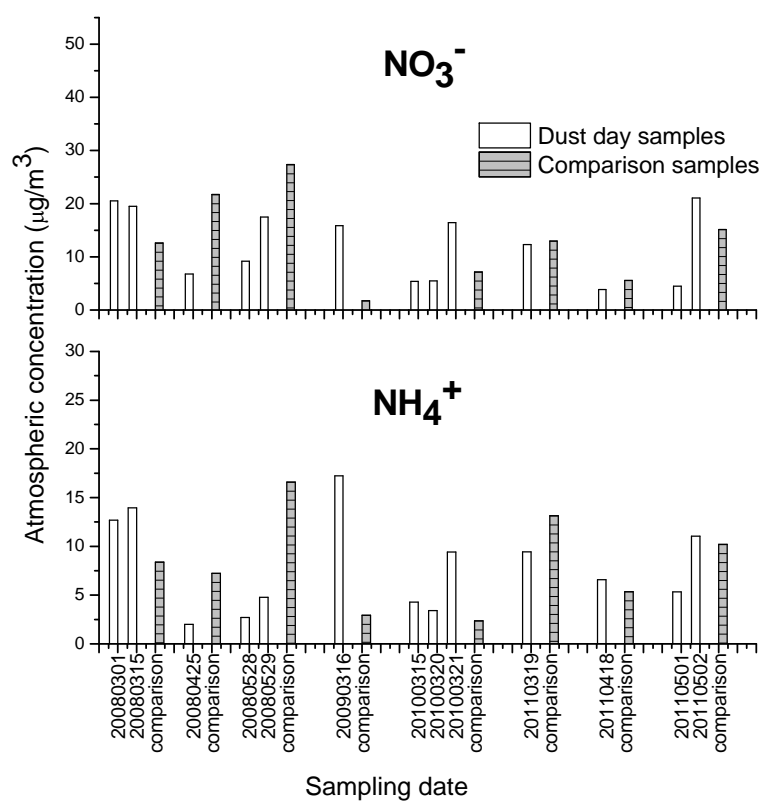


域代码已更改

1349
 1350
 1351
 1352
 1353
 1354
 1355
 1356

Figure 3. Mass concentrations of TSP, Al, Fe and nss-Ca in aerosol samples collected at the Baguanshan site on dust and comparison days from 2008-2011.

1357
 1358
 1359
 1360
 1361
 1362
 1363
 1364
 1365
 1366
 1367

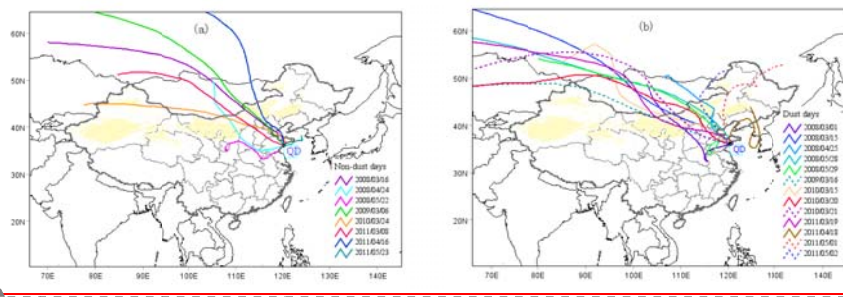


域代码已更改

1368
 1369
 1370
 1371
 1372
 1373
 1374
 1375
 1376
 1377

Figure 4. Mass concentrations of NH₄⁺ and NO₃⁻ in aerosol samples collected at the Baguanshan site on dust and comparison days during March-May in 2008 to 2011.

1379
1380
1381
1382
1383
1384
1385
1386
1387
1388
1389
1390



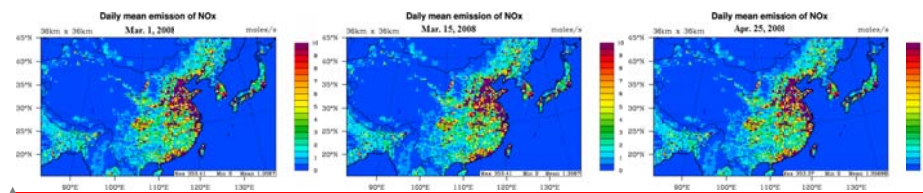
带格式的: 字体: (默认) Times
New Roman, 字体颜色: 红色

1391
1393
1394
1394
1395
1396
1397
1398
1399
1400
1401
1402
1403
1404
1405
1406
1407
1408
1409
1410
1411
1412
1413
1414

Figure 5. The 72-h backward trajectories for non-dust (a) and dust (b) samples from 2008 to 2011 (the yellow domains in the maps represent the dust source regions in China).

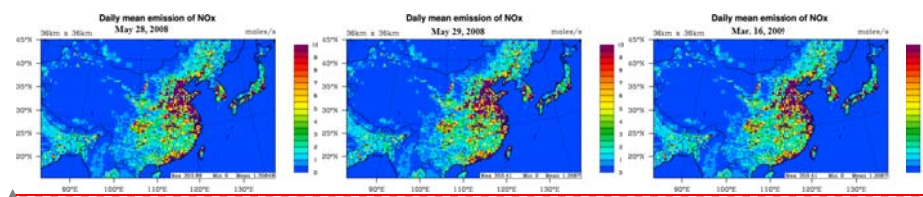
1415
1416
1417
1418
1419
1420
1421
1422
1423
1424
1425
1426

1427



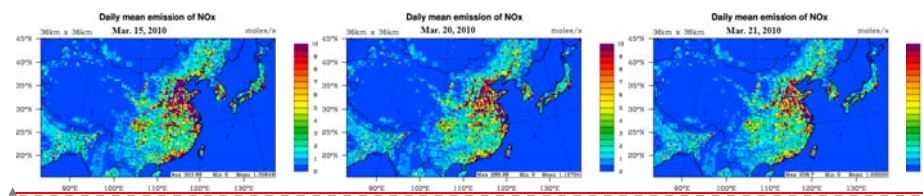
带格式的: 字体: (默认) Times New Roman

1428



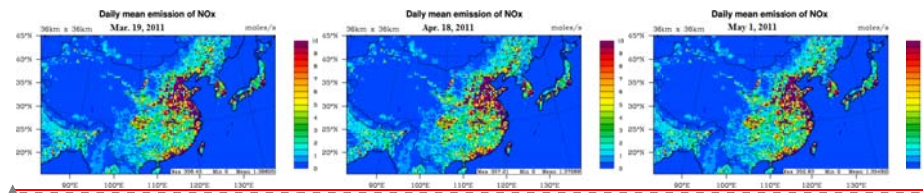
带格式的: 字体: (默认) Times New Roman

1429



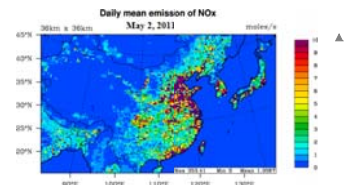
带格式的: 字体: (默认) Times New Roman

1430



带格式的: 字体: (默认) Times New Roman

1432



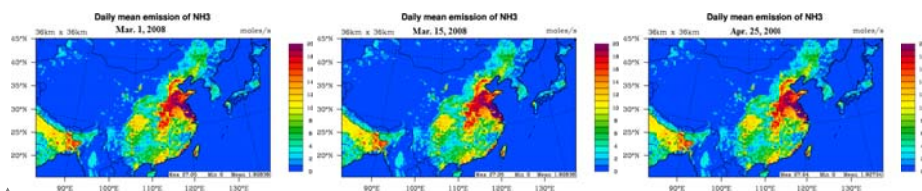
带格式的: 字体: (默认) Times New Roman

1433

1434

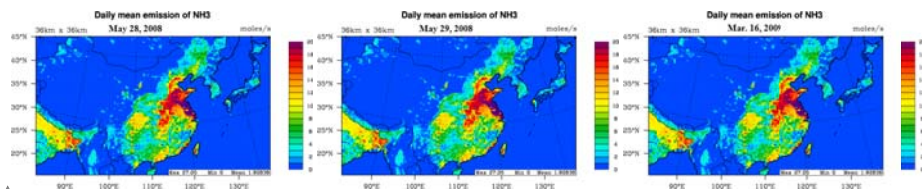
Figure 6. Daily mean emission of NOx over East Asia on the dust days from 2008 to 2011.

1435
1436
1437
1438
1439
1440
1441
1442
1443



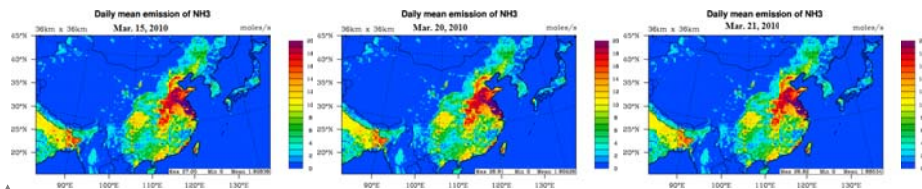
带格式的: 字体: (默认) Times New Roman, 小五

1444



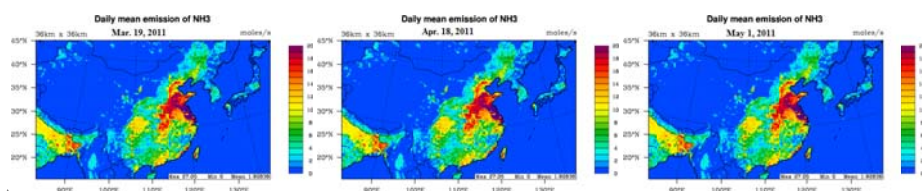
带格式的: 字体: (默认) Times New Roman, 小五

1445



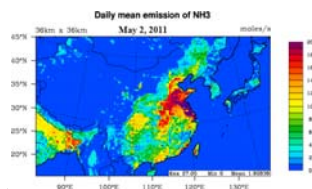
带格式的: 字体: (默认) Times New Roman, 小五

1446



带格式的: 字体: (默认) Times New Roman, 小五

1447



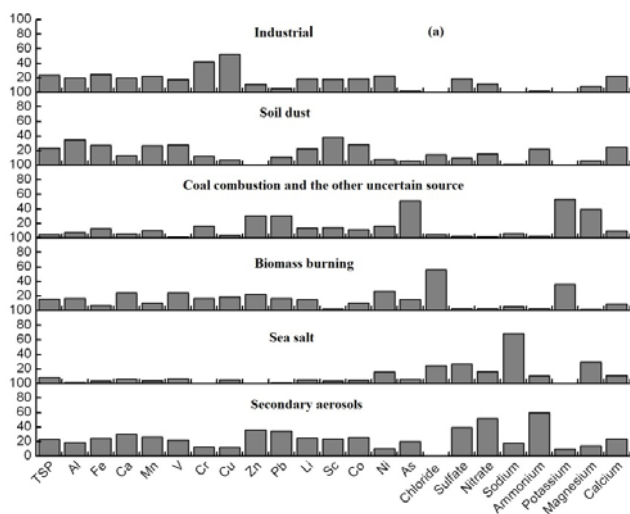
带格式的: 字体: 小四

1448

1449 **Figure 7.** Daily mean emission of NH₃ over East Asia on the dust days from 2008 to 2011.

1450
1451

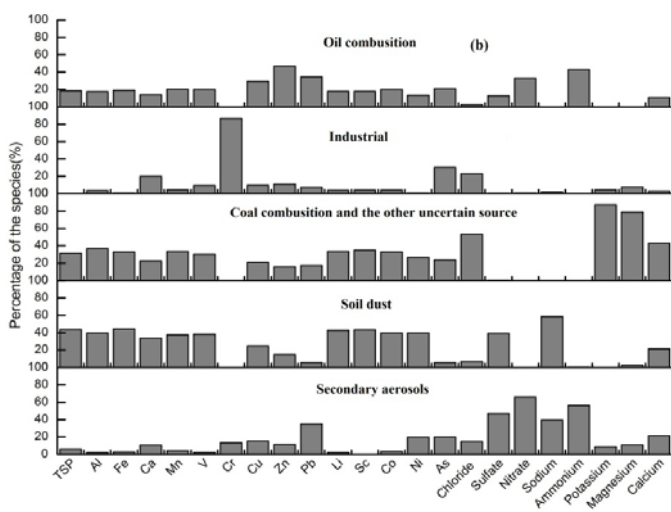
1451
1452
1453
1454
1455
1456
1457
1458
1459



带格式的: 字体: (默认) Times
New Roman, 10 磅

带格式的: 缩进: 首行缩进: 1 字
符

1460



带格式的: 字体: (默认) Times
New Roman, 10 磅

1461

1462

1463

1464

1465

Figure 8. Source profiles of atmospheric aerosol samples collected on non-dust (a) and dust (b) days using the PMF model

带格式的: 行距: 1.5 倍行距

页 24: [1] 带格式的	微软用户	2017/6/19 15:53:00
----------------	------	--------------------

字体: 10 磅

页 24: [1] 带格式的	微软用户	2017/6/19 15:53:00
----------------	------	--------------------

字体: 10 磅

页 24: [2] 带格式的	微软用户	2017/6/19 15:53:00
----------------	------	--------------------

字体: 10 磅

页 24: [2] 带格式的	微软用户	2017/6/19 15:53:00
----------------	------	--------------------

字体: 10 磅

页 24: [2] 带格式的	微软用户	2017/6/19 15:53:00
----------------	------	--------------------

字体: 10 磅

页 24: [2] 带格式的	微软用户	2017/6/19 15:53:00
----------------	------	--------------------

字体: 10 磅

页 24: [2] 带格式的	微软用户	2017/6/19 15:53:00
----------------	------	--------------------

字体: 10 磅

页 24: [2] 带格式的	微软用户	2017/6/19 15:53:00
----------------	------	--------------------

字体: 10 磅

页 24: [2] 带格式的	微软用户	2017/6/19 15:53:00
----------------	------	--------------------

字体: 10 磅

页 24: [2] 带格式的	微软用户	2017/6/19 15:53:00
----------------	------	--------------------

字体: 10 磅

页 24: [2] 带格式的	微软用户	2017/6/19 15:53:00
----------------	------	--------------------

字体: 10 磅

页 24: [2] 带格式的	微软用户	2017/6/19 15:53:00
----------------	------	--------------------

字体: 10 磅

页 24: [2] 带格式的	微软用户	2017/6/19 15:53:00
----------------	------	--------------------

字体: 10 磅

页 24: [2] 带格式的	微软用户	2017/6/19 15:53:00
----------------	------	--------------------

字体: 10 磅

页 24: [2] 带格式的	微软用户	2017/6/19 15:53:00
----------------	------	--------------------

字体: 10 磅

页 24: [2] 带格式的	微软用户	2017/6/19 15:53:00
----------------	------	--------------------

字体: 10 磅

页 24: [3] 带格式的	微软用户	2017/6/19 15:53:00
----------------	------	--------------------

字体: 10 磅

页 24: [3] 带格式的	微软用户	2017/6/19 15:53:00
----------------	------	--------------------

字体: 10 磅

页 24: [3] 带格式的	微软用户	2017/6/19 15:53:00
----------------	------	--------------------

字体: 10 磅

页 24: [3] 带格式的	微软用户	2017/6/19 15:53:00
----------------	------	--------------------

字体: 10 磅

页 24: [3] 带格式的	微软用户	2017/6/19 15:53:00
----------------	------	--------------------

字体: 10 磅

页 24: [3] 带格式的	微软用户	2017/6/19 15:53:00
----------------	------	--------------------

字体: 10 磅

页 24: [3] 带格式的	微软用户	2017/6/19 15:53:00
----------------	------	--------------------

字体: 10 磅

页 24: [3] 带格式的	微软用户	2017/6/19 15:53:00
----------------	------	--------------------

字体: 10 磅

页 24: [3] 带格式的	微软用户	2017/6/19 15:53:00
----------------	------	--------------------

字体: 10 磅

页 24: [3] 带格式的	微软用户	2017/6/19 15:53:00
----------------	------	--------------------

字体: 10 磅

页 24: [3] 带格式的	微软用户	2017/6/19 15:53:00
----------------	------	--------------------

字体: 10 磅

页 24: [3] 带格式的	微软用户	2017/6/19 15:53:00
----------------	------	--------------------

字体: 10 磅

页 24: [3] 带格式的	微软用户	2017/6/19 15:53:00
----------------	------	--------------------

字体: 10 磅

页 24: [4] 带格式的	微软用户	2017/7/11 13:17:00
----------------	------	--------------------

字体: (默认) Times New Roman, 10 磅

页 24: [4] 带格式的	微软用户	2017/7/11 13:17:00
----------------	------	--------------------

字体: (默认) Times New Roman, 10 磅

页 24: [4] 带格式的	微软用户	2017/7/11 13:17:00
----------------	------	--------------------

字体: (默认) Times New Roman, 10 磅

页 24: [4] 带格式的	微软用户	2017/7/11 13:17:00
----------------	------	--------------------

字体: (默认) Times New Roman, 10 磅

页 24: [4] 带格式的	微软用户	2017/7/11 13:17:00
----------------	------	--------------------

字体: (默认) Times New Roman, 10 磅

页 24: [5] 带格式的	微软用户	2017/7/11 13:19:00
----------------	------	--------------------

字体: (默认) Times New Roman, 10 磅

页 24: [5] 带格式的	微软用户	2017/7/11 13:19:00
----------------	------	--------------------

字体: (默认) Times New Roman, 10 磅

页 24: [5] 带格式的	微软用户	2017/7/11 13:19:00
----------------	------	--------------------

字体: (默认) Times New Roman, 10 磅

页 24: [5] 带格式的	微软用户	2017/7/11 13:19:00
----------------	------	--------------------

字体: (默认) Times New Roman, 10 磅

页 24: [5] 带格式的	微软用户	2017/7/11 13:19:00
----------------	------	--------------------

字体: (默认) Times New Roman, 10 磅

页 24: [5] 带格式的	微软用户	2017/7/11 13:19:00
----------------	------	--------------------

字体: (默认) Times New Roman, 10 磅

页 24: [5] 带格式的	微软用户	2017/7/11 13:19:00
----------------	------	--------------------

字体: (默认) Times New Roman, 10 磅

页 24: [5] 带格式的	微软用户	2017/7/11 13:19:00
----------------	------	--------------------

字体: (默认) Times New Roman, 10 磅

页 24: [5] 带格式的	微软用户	2017/7/11 13:19:00
----------------	------	--------------------

字体: (默认) Times New Roman, 10 磅

页 24: [5] 带格式的	微软用户	2017/7/11 13:19:00
----------------	------	--------------------

字体: (默认) Times New Roman, 10 磅

页 24: [5] 带格式的	微软用户	2017/7/11 13:19:00
----------------	------	--------------------

字体: (默认) Times New Roman, 10 磅

页 24: [5] 带格式的	微软用户	2017/7/11 13:19:00
----------------	------	--------------------

字体: (默认) Times New Roman, 10 磅

页 24: [5] 带格式的	微软用户	2017/7/11 13:19:00
----------------	------	--------------------

字体: (默认) Times New Roman, 10 磅